Master of Science Dissertation

VT2013

Robustness of the voluntary breath-hold approach for the treatment of early stage lung cancer with spot scanned proton therapy

Jenny Dueck

Supervision
Per Munck af Rosenschöld, Antje Knopf, Tony Lomax

This work has been conducted at
Department of Medical Radiation Physics, Clinical Sciences, Lund University, Lund, Sweden.
Department of Radiation Oncology, Rigshospitalet (Copenhagen University Hospital), Copenhagen, Denmark
Center of Proton Therapy, Paul Scherrer Institut, 5232 Villigen PSI, Switzerland

Department of Medical Radiation Physics,
Clinical Sciences, Lund
Lund University

Advisors

Francesca Albertini, PhD
Mirjana Josipovic, MSc, MPE
Marianne Aznar, PhD
Gitte Persson, MD, PhD
Svend Aage Engelholm, MD, PhD, Professor

Acknowledgements

I would like to thank my supervisor Per Munck af Rosenschöld for his support and guidance during the project, and for his advice and ideas. I would also like to thank my supervisor Antje Knopf for her support and advice, and a special thank for the deformable image registration with 4D calculations, which I know was time consuming. I would like to thank my supervisor Tony Lomax for fruitful discussions and for giving me the opportunity to work at PSI during this project. Thanks also to Francesca Albertini for helping me with the treatment planning system, for clinical advice and also for the help to arrange the stay at PSI.

Thanks for the support and ideas to Mirjana Josipovic, Marianne Aznar, Gitte Persson and Svend Aage Engelholm at Rigshospitalet together with Ye Zhang and Stefano Gianolini at PSI. Thanks also to additional persons at PSI and Rigshospitalet who made this project feasible.

Finally, I would like to thank my professors and teachers at Lund University for interesting and inspiring classes and lectures. I would also like to thank my classmates for their kindness, support and fruitful discussions during the last five years.

Jenny

Table of contents

1 ABSTRACT

Background: Intra- and interfractional variations in anatomy can cause unplanned substantial alterations of the dose distribution of the target in proton therapy. Motion management methods might be used in order to minimize anatomical variations. In the proton therapy of lung cancer, a potential motion management technique is the use of the voluntary breath-hold approach. The aim of this study was to investigate the robustness of proton therapy treatment plans of lung cancer towards interfractional variations using voluntary breath-hold.

Materials and methods: Fifteen patients previously treated for Non-Small Cell Lung Cancer (NSCLC) or lung metastases with Stereotactic Body Radiation Therapy (SBRT) were included in this study. A voluntary breath-hold CT scan was collected as a part of the planning procedure and following each treatment fraction. The purpose of this treatment planning study was to obtain treatment plans for all the patients and then recalculate these on the repeated breath-hold CT scans, in order to investigate the robustness of the voluntary breath-hold approach. We used the definition of robust being as if the volume of the target receiving 95% of the prescribed dose (V95%) deviated less than 5% during the treatment. Two different plans were made; 2F with two fields and 3F with three fields. The Dose Volume Histogram (DVH) was evaluated for the Gross Target Volume (GTV), the Planning Target Volume (PTV), and the Organs at Risk (OAR) after both a Rigid Image Registration (RIR) recalculation and a Deformable Image Registration (DIR) recalculation of the treatment plans.

Results: The results of the study shows that after a RIR recalculation 6/15 (2F) and 9/15 (3F) treatments passed our robustness criterion. For two different DIR recalculations, 9/15 (3F) treatments for the first one and 3/4 (2F) and 2/4 (3F) treatments for the second one also passed our robustness criterion. The study further shows that the robustness was associated with the size of the target, with the slope of the regression curve being significant. No difference in robustness with respect to the number of fields per plan (two or three) was found.

Discussion: The results of this study show that for a majority of the cases the voluntary breath-hold approach seems robust. It may be necessary to have a cut off for small targets, as the robustness correlates with the size. Small tumors should be studied in more detail in future investigations. Remaining intrafractional motion during the treatment and the breath-holds, which was not considered in this study, may further compromise the robustness of the approach.

2 SWEDISH POPULAR SCIENTIFIC ABSTRACT/ SVENSK POPULÄRVETENSKAPLIG SAMMANFATTNING

En behandlingsmetod för lungcancer som blir mer och mer vanlig idag är protonterapi. Protonterapi fungerar på liknande sätt som vanlig strålbehandling med fotoner, med vissa skillnader. Protonterapi kan i princip minska biverkningarna av behandlingen jämfört med fotoner eftersom man med protonterapi bättre kan undvika den friska vävnaden. Ett stort problem med protonterapi är dess känslighet för rörelse under och mellan behandlingarna (s.k. intra- och interfraktionell rörelse). Det finns olika tekniker för att handskas med dessa rörelser; både tekniker som begränsar rörelserna, och tekniker som tar hänsyn och även korrigerar behandlingen efter rörelserna. En speciellt viktig intrafraktionell rörelse är andningen. En teknik som minskar andningsrörelserna är breath-hold-tekniken (sv. ”hålla andan”). I denna teknik får patienterna hålla andan under tiden behandlingen ges. Denna studie går ut på att undersöka stabiliteten för breath-hold tekniken. Femton tidigare behandlade patienter med lungcancer är inkluderade i denna studie. De har genomgått CT-undersökningar i samband med förberedelserna inför behandlingen samt vid varje behandlingstillfälle. Denna studie går ut på att göra behandlingsplaner för varje patient som sedan kan appliceras på de upprepade CT-bilderna som tagits under behandlingens gång. Resultatet av detta kan ge svar på hur den dosimetriska effekten är av denna teknik.

Behandlingsplanerna räknas om efter att CT-bilderna har blivit registrerade (matchade) till varandra med både en rigid registrering och en deform registrering. Den rigida registreringen tar bara hänsyn till patientens fasta rörelse och inte rörelser organen sinsemellan eller tillväxt/minskning av target (målvolymen, tumören). Den deforma registreringen som tar hänsyn till det nyss nämnda deforma rörelsemönstret resulterar således i en bättre utvärderingsmetod. Det kan dock finnas problem med dessa algoritmer i dagsläget som gör att den rigida registreringen ändå eventuellt speglar en mer korrekt bild av dosfördelningen.

Resultaten visar att dosfördelningen av target är lika eller tillräckligt lika den som var planerad från början för en majoritet av patienterna. Detta tyder på att breath-hold tekniken är stabil. Man fann också att stabiliteten i behandlingen beror på storleken av target. Var man ska sätta gränsen för hur små target som kan behandlas, får kommande studier visa.

Det är även intressant att i framtiden studera hur intra-/interfraktionella rörelser kan påverka behandlingens stabilitet och hur man kan öka reproducerbarheten i andetagen för att på sätt öka stabiliteten för breath-hold tekniken.

3 INTRODUCTION

Radiation therapy is presently an important component of the management of cancer patients, typically in combination with surgery and/or chemotherapy. Most common is the radiation therapy with photons, but both ion therapy and particularly proton therapy are techniques expanding to more and more facilities around the world.

In terms of biological effect on tissues, the radiation therapy using photons and protons are rather similar, whilst differences of the deposition of radiation dose due to the physical properties of photons and protons are substantial. For photons, the absorbed dose decreases with the water equivalent depth, while for protons the absorbed dose increases and then decreases rapidly to almost zero at a certain depth. This peak of the depth dose curve is called the Bragg peak and is the main advantage of proton therapy (Pedroni *et al.*, 1995). In radiation therapy, the Bragg peak can be used to limit the integral dose (the total energy deposited in tissue) as compared to photon treatment (i.e. the dose distribution of the target is more conformal for proton therapy). An example of a Bragg peak is shown in Figure 1, measured at a QA session at Gantry 1, Paul Scherrer Institut (PSI), Switzerland 2013-04-05. Here one can see that for the energy of 160 MeV the protons have a range of almost 18 cm in water equivalent material. Note also the fast distal fall off of the relative dose.

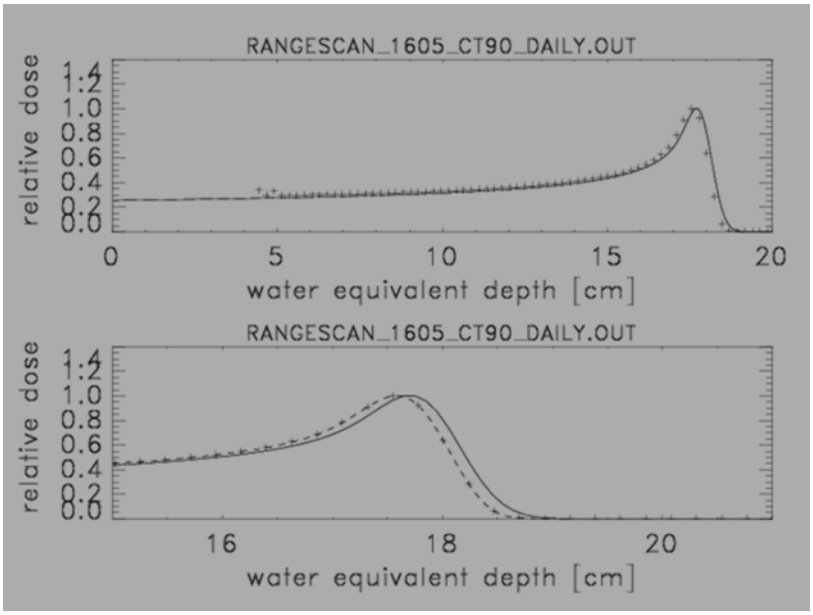

Figure 1. The relative dose as a function of the water equivalent depth from the daily QA 2013-04-05 at Gantry 1, PSI, Switzerland, with 160MeV as initial energy. The peak is called the Bragg peak. The lower figure is an enlargement of the Bragg peak in the upper figure. The dotted line is the measurements at the session and the solid line is the commissioning data for the Gantry (the look up table).

Patients with lung cancer have unfortunately a very poor survival rate today. In United States of America (USA) the relative five year survival rate for patients with cancer seated in lung or bronchus is only 16% (Siegel *et al.*, 2013). In Sweden the same number is 12% for men and 15% for women (Cancerfonden, 2009). For localized and thereby early stage lung cancer the five year survival rate in USA is 52% (Siegel *et al.*, 2013), which indicates the need of a treatment with a low rate of complications and late effects.

One way of increasing the local control of the disease and possibly the survival rate may be to increase the prescribed dose (Robertson *et al.*, 1997; Rosenzweig *et al.*, 2000). Robertson *et al.* states that the risk of developing radiation pneumonitis is the limiting factor when aiming to increase the prescribed dose. Since proton therapy can deliver more conformal treatment plans, one might be able to increase the prescribed dose compared to the dose in photon therapy without increasing the probability of radiation pneumonitis. Nevertheless, regardless of cancer type the proton therapy treatment can spare more normal tissue and hence decrease the complication risk compared to photon treatment. In addition, radiation induced pneumonitis has been shown to be associated with the dose to the heart (Huang et al., 2011), which can be limited using proton therapy. An important issue in proton therapy is the risk of low robustness of the treatments because of motion of the tumor (target). This will be explained in detail later.

3.1 RADIATION THERAPY

The aim of radiation therapy is to treat cancer by damaging the tumor while sparing the surrounding normal tissue.

To be able to investigate and later optimize the absorbed doses to the patients prior the treatment, a treatment plan has to be constructed with the help of a treatment planning system based on images of the patient acquired by a Computed Tomography scan (CT scan). Also Positron Emission Tomography (PET) and/or Magnetic Resonance Imaging (MRI) may be used as planning tools depending on indication. For lung cancer, FDG PET (PET scan with the radiopharmaceutical ^{18}FDG) is routinely used in the staging and target definition prior to the radiation therapy.

The International Commission on Radiation Units and Measurements (ICRU) has defined useful tools and concepts in radiation therapy. In ICRU report 78 and 83 (ICRU, 2010, 2007) a set of volumes of interest when making a treatment plan is defined. The target consists of three sub volumes (see Figure 2). The Gross Tumor Volume (GTV) is the volume of the tumor visible on diagnostic imaging (e.g. CT, MR, PET, US (Ultrasound)) and/or palpable by the physician. The Clinical Target Volume (CTV) encloses the GTV with a margin to enclose microscopic tumor cells below the detection limit of the imaging modalities and is decided by the physician based on clinical experience. The Planning Target Volume (PTV) is the volume enclosing the CTV and with a margin to account for uncertainties in the radiation delivery. These uncertainties can be due to setup-, dosimetric- or machine uncertainties, or due to motion of the target caused by for example breathing. Furthermore, to be able to investigate and optimize the dose to the surrounding organs, the physicians also delineate the Organs At Risks (OARs) in the treatment planning system.

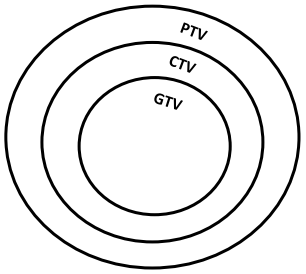

Figure 2. The volumes of the target (schematically). The Gross Target Volume (GTV) is enclosed in the Clinical Target Volume (CTV) which is enclosed in the Planned Target Volume (PTV).

The aim of the treatment planning process is two-fold. Firstly, the treatment planner strive to arrive with a plan that deliver a homogenous dose, as defined by ICRU, where the dose in PTV is within -5 and +7% deviation from the prescribed dose (ICRU, 2010, 2007). Secondly, the optimal plan should avoid the dose to OAR structures as much as possible. Finally, during the treatment planning evaluation phase the physician evaluates and approves the absorbed dose distribution to the OARs and the target volumes before the start of the treatment.

The above described definitions and procedures are valid for both photon and proton therapy. From now on only proton therapy will be discussed.

3.2 BEAM DELIVERY

The protons are generated in either a synchrotron or a cyclotron. Basically, the difference between these two accelerators is that protons of *different* energy and *the same* intensity can be generated by the synchrotron, while protons with *the same* energy and *different* intensity can be generated by the cyclotron

Slow protons are inserted into the synchrotron and accelerated to a fixed energy in the range of 80-250 MeV (Schippers, 2011). An advantage of the synchrotron is that it can deliver any energy of the protons in the above mentioned range. The synchrotron can then theoretically produce protons with different energy during the treatment. More commonly is the output of mono-energetic protons which are energy-degraded by physical range modulators, i.e. materials in the line of the beam.

The cyclotron can produce protons of a fixed energy of most commonly 230 or 250 MeV (Schippers, 2011). The protons are produced by ionizing hydrogen gas and then accelerated in the cyclotron with the help of magnets and radio frequent pulses. The intensity of the beam can be changed rapidly to fit the clinical acquirements.

From a cyclotron the beam needs to be energy degraded into the clinical acquirements, usually by tissue equivalent material inserted into the beam. To compensate for the loss in beam quality, collimators, slits and magnets can be used. The beam is then transported through a system in vacuum into the treatment room. To ensure the beam quality along the beam transportation, several magnets can be used. Depending on which delivery technique is used (see Section Passively scattered proton therapy and Section Scanned proton therapy), the transport of the protons through the gantry and nozzle of the treatment delivery system will be different. In general one can say that the protons go through equipment such as beam diagnostics equipment

(e.g. ionization monitors), range modulators and compensators in the nozzle (which is mounted on the either static or rotating gantry) before the beam will reach the snout (the head of the nozzle) and eventually the patient (Zuofeng *et al.*, 2011).

The proton beam delivered by the synchrotron or the cyclotron is a narrow mono-energetic pencil beam of protons. The beam size in the orthogonal direction of the beam is much smaller than the size of a common target. For example the Gantry 1 at PSI, Switzerland produces a beam that is 8 mm Full Width at Half Maximum (FWHM) in the focus point (Lomax *et al.*, 2004). The goal of the therapy is to deliver dose to the entire target. There are currently two kinds of techniques to achieve dose to the entire target; passively scattered proton therapy and scanned proton therapy.

3.2.1 PASSIVELY SCATTERED PROTON THERAPY

In passively scattered proton therapy there are high-z-materials (scattering foils) placed in the beam line, which by scattering broadens the proton beam. Because only the most centered part of the scattered beam is useful (because of low intensity in the edges), for large targets double foils are used rather than one single foil (Miller, 1995). By the use of collimators and compensators one can modulate the beam into any shape of the distal edge of the target in the beams eye view.

To change the energy of the beam and thereby also the range of the protons, range modulation devices are used, often a range modulator wheel with various thicknesses. With the use of these range modulators the narrow Bragg peak becomes a (in the direction of the beam) wider Spread Out Bragg Peak (SOBP).

3.2.2 SCANNED PROTON THERAPY

The objective of this technique is, as the name suggests, a narrow pencil beam which is being scanned across the target. For example, at Gantry 1 at PSI the beam is scanned with a magnet in one direction while the treatment couch is moving in the other direction to deliver a two-dimensional dose distribution (Lomax *et al.*, 2004). The dose distribution can be expanded to three dimensions by the use of range shifters. The range shifters for scanned proton therapy results in, in contrast to the passively scattered proton therapy, discrete energy step (Miller, 1995). With this technique one can "place" the Bragg peaks on various positions in the target to get a uniform dose distribution. If these Bragg peaks are discretely placed, it is called *spot* scanning, in contrast to the *dynamic* scanning technique.

The main advantage of the scanned proton therapy compared to passively scattered proton therapy, is the more conformal treatment plans and that there are no use of patient specific equipment like compensators or collimators. Another advantage is the low production of neutrons during the treatment and thereby a lower integral dose to the patient (Hall, 2006).

The scanning technique allows types of treatment plans namely Single Field, Uniform Dose (scanning beam SFUD) plans and Intensity Modulated Proton Therapy (IMPT) plans. The difference between these two techniques is that for SFUD treatment plans the weight of the Bragg peaks are optimized to make every treatment field homogenous, whilst for IMPT treatment plans the weight of the Bragg peaks are optimized to make the total dose distribution homogenous (Lomax, 1999). In IMPT treatment plan optimization one can also define dose constraints of both target and OARs.

The most common treatment plans are the SFUD plans. The fact that every field is homogenous makes the treatment plans robust to movements of the target during the treatment. These SFUD treatment plans can be delivered with either passively scattered beams or with scanned beams while IMPT treatment plans in the sense as described by Lomax (Lomax, 1999) can only be delivered with scanned beams.

3.3 MOTION OF THE TARGET

As mentioned before, the target may move during the treatment. This can result in unwanted "hot spots" or "cold spots" in the dose distribution of the target, or a smearing out of the dose distribution leading to a worse target coverage. One way of coping with this motion is the use of PTV as previously described (to cope with the smearing out of the dose distribution), but there are more techniques available to reduce, control or monitor the movements (to also cope with the "hot spot" and "cold spots").

When treating a tumor located in a part of the body that is presumably static there are yet uncertainties in the delivery of the beam. These uncertainties come from for example setup errors of the patient. With the positioning technique today with immobilization devices (e.g. cushions and masks) and image acquisition before and during treatment, these setup errors can be minimized. When treating a moving target it is more complicated. Besides the effect of target under dosage because of the smeared out dose distribution in the presence of movement, for proton therapy the density variations affect the range of the protons. This means that if there are large density variations in front of the target, the protons may not reach the target at all or may go too far and reach the normal tissue beyond to the tumor. Because of this it is not only important to investigate the motion of the target, but also the motion of all structures in the radiation field to reassure that the treatment will be delivered as planned.

For scanned proton therapy there is an additional effect caused by motion; the interplay effect. If the delivery of the scanned pencil beams moves with the same time resolution as the movement of the target (caused by e.g. breathing) there will be an interplay effect of the movement of the beam and the target. This can lead to severe under or over dosages of the target and the OAR respectively. Furukawa *et al.* simulated this interplay effect and in the simulations the deteriorated dose distribution could be demonstrated (Furukawa *et al.*, 2010).

Proton facilities with the scanning beam technique need to do very careful investigations before treating moving targets or even refrain from treating them at all, because of these three above mentioned reasons (dose distribution can be smeared out, range changes of the protons and interplay effects).

3.3.1 DIFFERENT TYPES OF MOTION

Even if immobilization devices are used and the patient is supposed to lie perfectly still during the treatment, there can be some residual motion of the target; this motion constitutes the intrafractional motions. Intrafractional motions are movements that can occur during the irradiation/treatment. It can be for example breathing, swallowing and/or heartbeats, but also bladder and rectum filling and bowel movements. These motions are not easy to monitor since they occur during the delivery of the treatment.

Interfractional motions, on the other hand, are movements that can occur between the treatment fractions, including e.g. weight loss/gain of the patient and shrink/growth of the tumor. To avoid deviations of the planned dose distributions one can monitor these changes by

imaging devices in the treatment room, by repeated treatment simulations and/or by the use of extra margins from CTV to the PTV.

3.4 RADIATION THERAPY MOTION MANAGEMENT OF LUNG CANCER

There are several ways of dealing with targets that are moving because of breathing. Either one can try to reduce the movement itself by e.g. introducing a breath-hold, or one can try to monitor the motion during the treatment and adjust the treatment from the gained information (e.g. tracking and gating) (Keall *et al.*, 2006). To only cope with the smeared out dose distribution one can investigate the motion during free breathing and increase the margin between the CTV and the PTV depending on the magnitude of the tumor movement. The latter technique requires access to a 4DCT scan of the patient.

3.4.1 BREATH-HOLD

There are various techniques for the use of the breath-hold approaches which varies in reproducibility uncertainties and patient comfort. Whilst self-held or voluntary breath-holds are the most comfortable for the patient it is also the most uncertain strategy. To increase the reproducibility of the breath-holds one can use a respiratory monitoring system and/or coaching of the patient during the treatment. A technique with a theoretically low uncertainty is the Active-Breathing Control (ABC) where the patient has an assisted breath-hold using a valve controlled spirometer. This can be of higher discomfort for the patient. The breath-hold can be held in the inspiration, the expiration or in the middle phase of the respiratory cycle. An advantage of the Deep Inspiration Breath-Hold (DIBH) technique is that the inflation of the lung may give a dosimetric advantage as a relatively smaller part of the lung is within the treatment field.

If the delivery of the irradiation is rapid maybe the entire field or treatment can be delivered in one single breath-hold. Otherwise the patient has to repeat the breath-hold several times per treatment, thereby decreasing the robustness of the treatment if the reproducibility of the breath-hold is not optimal.

The DIBH approach is used in studies by Hanley *et al.* and Rosenzweig *et al.* where they use the ABC system (Hanley *et al.*, 1999; Rosenzweig *et al.*, 2000). In the study by Hanley *et al.* they found the reproducibility of the DIBH technique to be 1.0 ± 0.9 mm intra breath-hold and 2.5 ± 1.6 mm inter breath-hold. Further, they found out that the volume of the lung receiving 25 Gy decreased with 30% in comparison with the free breathing technique. The patients could hold their breath for 12-16 seconds and repeat it 10-13 times during the treatment.

3.4.2 GATING

A technique to monitor the movement of the target instead of controlling it, is the respiratory gating technique. This technique allows the radiation to be delivered only in a predefined phase of the breathing cycle. This predefined phase could be for example in the end of the expiration or the inspiration phase. The breathing of the patient is monitored by a gating system which is connected to the CT scan and the gantry to gate the CT acquisition and the treatment respectively.

This technique was suggested over twenty years ago by e.g. Philips *et al.*, as a way of dealing with motion in charged particles therapy with spot scanning (Phillips *et al.*, 1992). In the article it was also suggested to use rescanning as a way of smoothing the otherwise inhomogeneous dose distribution caused by the interplay effect.

Like for all patient monitoring systems used for respiratory gating or breath-hold, a good indicator of the tumor position and motion is necessary (e.g. a part of the surface as seen by a camera, the changes in abdomen pressure during breathing (Vasquez *et al.*, 2012) or measurements of the lung volume by a spirometer (Hanley *et al.*, 1999; Rosenzweig *et al.*, 2000)) and it is important that one can relate the motion of the marker with good certainty to the tumor.

3.4.3 RESCANNING

If one already uses a technique to cope with the movement of the tumor and the density changes, the rescanning approach is a way to deal with the residual interplay effect. As mentioned above the effects of a beam moving with the approximately same velocity as the target movement, can be under dosage of the target and over dosage of the OARs. When using rescanning one delivers the radiation over the same area many times to smooth out the dose distribution and by that decrease the over and under dosages.

Knopf *et al.*, investigated the effect of motion in the dose distribution in relation to the number of fields and also the effect if using rescanning (Knopf *et al.*, 2011). They found that the effect of motion decreases with the number of fields, because the delivery of multiple fields is in itself a way of rescanning. The rescanning improves further the quality of the plan the most for a small number of fields. This implies that fewer rescans are necessary for plans with multiple fields. They also found that the number of rescans and the homogeneity is not a linear dependency, thus one have to pay attention to the choice of the number of the rescans.

At PSI, the Gantry 2 that is not yet in clinical use, is going to be able to deliver treatment plans with rescanning to moving targets. The plan is to be able to deliver a 2 Gy treatment fraction to a target of 1 liter with 10 rescans in about 2 minutes (Knopf *et al.*, 2011).

3.4.4 TRACKING

A fourth way of dealing with motion is tracking, where the movement of the tumor is tracked during the treatment. This requires a method to observe the tumor in real time (e.g. fluoroscopy) but also a computer system that can receive position signals, analyze it and move the treatment field very fast.

van de Water *et al.*, investigated the tracking method (van de Water *et al.*, 2009). They found that the spot scanning together with the tracking technique are sensitive to position errors. For the tracking technique to deliver a homogenous dose distribution to the target, the setup errors need to be less than 1 mm. For the tracking technique combined with the rescanning (rescan factor of 4) however, the setup errors can be up to 3 mm without impairing the homogenous dose distribution. This is true only for homogenous targets; with heterogeneous targets it is more or less required to use rescanning to at all be able to deliver a homogenous dose distribution to the target. The tracking itself can namely worsen the homogeneity of the dose distribution because of the density changes and thereby differences in the range of the protons (van de Water *et al.*, 2009).

Another study by Munck af Rosenschöld *et al.* presented promising results of the real-time geometrical tracking for IMPT as a way of dealing with movements of targets larger than 1 cm (Munck af Rosenschold *et al.*, 2010). They also found that movements of targets smaller than 1 cm resulted in acceptable dose distributions without tracking.

3.5 AIM OF THE PROJECT

The aim of the project was to investigate the voluntary breath-hold approach for scanned proton SFUD treatment plans. The main aim was to investigate whether this technique is robust; with the robustness in this case defined as if the volume of the PTV that receives 95% of the prescribed dose (PTV V95%) for the treatment (both from day to day and also summed over the entire treatment) do not deviate more than 5% from the planned dose distribution. The robustness was investigated both after a Rigid Image Registration (RIR) recalculation and a Deformable Image Registration (DIR) recalculation of the treatment plans.

4 MATERIALS AND METHODS

4.1 PAUL SCHERRER INSTITUT

Paul Scherrer Institut (PSI) is a federal research facility in Switzerland. By having approximately an equivalent of 1400 full-time workers it is the largest research facility in the country. The main research topics are Matter and Materials, Human Health, Energy and Environment.

The research center consists of mainly four facilities; Swiss Light Source (SLS), Spallation Neutron Source (SINQ), Moun Source (SμS) and Swiss X-ray Free-Electron Laser (SwissFEL) where the latter is currently under construction. The SLS is a facility where materials can be X-rayed by synchrotron light down do a scale of nanometers. In the facility SINQ the scientists can examine new materials with neutrons. With the mouns at SμS one can determine the magnetic field inside materials. At last, the aim of the SwissFEL is to be able to "track the progress of extremely rapid processes" ((Paul Scherrer Institut, 2013-05-02).

Within the field of Human Health, PSI has a proton facility where some types of cancer diseases can be treated. The proton facility consists of three treatment rooms; one for the treatment of eye cancer (OPTIS2), one for head & neck cancers/static tumors (Gantry 1) and the third one being currently under construction (Gantry 2). Gantry 2 is meant to be able to treat not only static cases as head & neck but also, in the future, moving targets such as lung and liver cancer.

4.2 PATIENTS

Fifteen patients previously treated at Rigshospitalet, Copenhagen University Hospital, Denmark for Non-Small Cell Lung Cancer (NSCLC) or lung metastases were included in this study. They were treated with Stereotactic Body Radiation Therapy (SBRT) with a prescribed dose of 3x15Gy during the years of 2009 and 2010. The median age of the patients was 73 years with a range of 60 to 87 years. Following the treatment preparations prior to the treatment start and following the three treatment fractions, voluntary breath-hold CT scans was acquired. The patients were asked to hold their breath as long as it was comfortable and they were monitored with a position management system. If the breath-hold was not stable, the CT scan was retaken. More information about the patients and the CT acquisition can be found in the PhD thesis and an article of Persson (Persson, 2011; Persson *et al.*, 2013). The CT data was stored in DICOM-format.

The planning CT scan acquired prior to the treatment and the corresponding treatment plan are in this study referred to as Planning CT, and the repeated CT scans and recalculated plans as Day 1, Day 2 and Day 3 respectively. For various reasons, only twelve of the patients had all three repeated CT scan acquired. Two of them had two repeated scans, and one had only one repeated scan, in addition to the Planning CT scan.

All patients had markers implanted in the tumor. Nine patients had a Gold Ancher™ (Naslund Medical, Huddinge, Sweden) implanted with the dimensions of 0.28x20 mm. Five patients had a Visicoil™ (IBA Dosimetry, Bartlett, TN, USA) gold marker with dimensions 0.75x20mm and finally one patient had a complex helical platinum coil (Boston Scientific, Natick, MA, USA) with a length of 20 mm restrained (2x4x4 mm unrestrained) (Persson *et al.*, 2013).

Because the treatment planning system PSIplan cannot handle gold and platinum markers, due to an inaccurate calibration curve of the Hounsfield Unit (HU) and stopping power for these materials, and also because of artifacts in the CT scan, the marker was removed, i.e. the density

of the markers was changed to the density of the tumor. In some cases the marker was not inside of the tumor and the density was then changed to the density of the lung instead.

The sizes and location of the targets together with the diagnosis of the patients are displayed in Table 1. The diagnosis is defined as a TNM stage (Tumor, Node, Metastasis). The tumor locations are denoted e.g. RLL for right lower lobe and LUL for left upper lobe (M is medium). As one can see, three of the cases have multi targets. For the purpose of this study, only one target (the largest one) per patient was considered.

Table 1. The size of the targets. The mean of the size was 51 (8.6-169) cm^3 when only one target (the largest one) per patient was considered. The diagnosis is defined as a TNM stage (Tumor, Node, Metastasis).The tumor locations are denoted e.g. RLL for right lower lobe and LUL for left upper lobe (M is medium).

Patient	Volume PTV (cm^3)	Diagnosis	Tumour location
1	72	NSCLC, T2N1M0	RLL
2	32, 3.2 and12	NSCLC, T2N2M0	LUL, LUL, RUL
3	169 and 8.0	NSCLC, T3N1M0	RUL, Mediastinum anterior
4	24	NSCLC, T2N0M0	RUL
5	41	NSCLC, T2N0M0	RUL
6	93	NSCLC, T2N0M0	RUL
7	9.6	NSCLC, T1N0M0	LLL
8	11	NSCLC, T1N0M0	LLL
9	8.6	NSCLC, T1N0M0	RLL
10	12 and 6.0	NSCLC, T4N0M0	RLL, RML
11	57	C. renis metastasis	RLL
12	61	NSCLC, T2N0M0	RUL
13	107	NSCLC, T3N0M0	RLL
14	59	NSCLC, T1N0M0	LLL
15	10	NSCLC, T1N0M0	LLL

4.3 TREATMENT PLANNING

The CT scans in DICOM format was converted into "PSI format", suitable for the in-house developed treatment planning system PSIplan Version 7.4.1 at PSI, by the software VODCA Radiotherapy 5.3.1 (MSS Medical Software Solutions GmbH). Later on, the treatment plans from PSIplan was converted back into DICOM format using the same software to be able to perform some additional analyses (DIR_velocity, as described in the section Deformable image registration).

Delineation of target and OARs were made in the software VIRTOUS 4.6.8 of Sep 2008 (Heidelberg Clinical Cooperation Unit Radiotherapy) and in the treatment planning system Eclipse™ version 11.0 (Varian Medial System Inc, Palo Alto, USA). The delineation of the GTV was performed by a single radiation oncologist. The PTV was constructed by adding a 5 mm margin to the GTV in all directions. According to the clinical protocol in use at Rigshospitalet no CTV was used.

For each patient two treatment plans was made, with two (2F) and three fields (3F) respectively. The aim was to have coplanar fields separated by 90 and 45 degrees respectively for each plan, but this was not possible to achieve in all cases because of the geometry. The dose was in all cases normalized to the mean dose of the target. Example of treatment plans (patient 1) is shown in Figure 3.

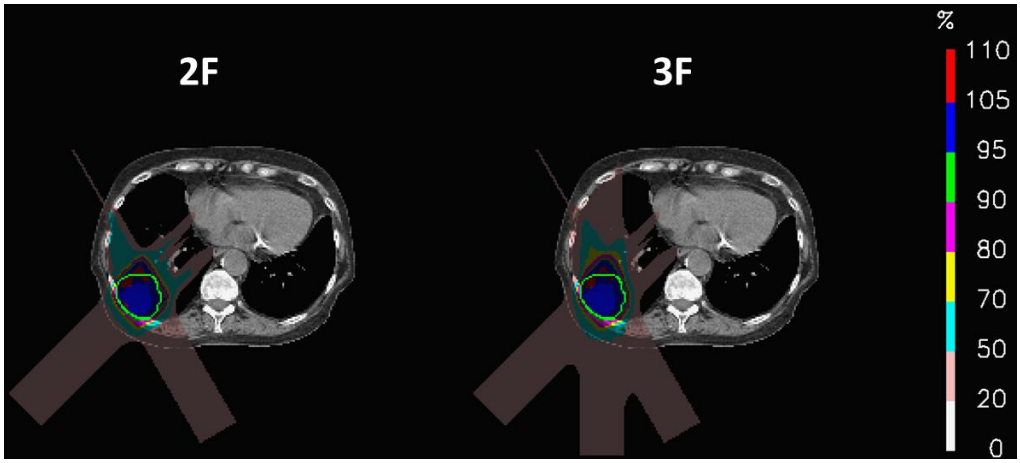

Figure 3. The treatment plans 2F (two fields) and 3F (three fields) for patient 1.

The clinical protocol in Copenhagen used to treat these patients was also used in this treatment planning study: the prescribed dose was 45 Gy to the PTV attempting to encompass the PTV with the 90-95% isodose line and attempting to keep the maximum to 107-110%. Treatments were delivered in three fractions. The dose constraints to the OARs are shown in Table 2. In the present work, the same dosimetric constraints were used but applied to the radiobiological corrected dose of the protons (D_{RBE} expressed as Gy(RBE)) where a weighting factor of 1.1 was used according to recommendations from ICRU (ICRU, 2007). Only the heart, spinal cord and lungs are considered in this work. In this work, we have strived to achieve a homogenous dose distribution inside the target. This is practical for the purpose of this study but necessarily not the best approach for SBRT of lung cancer, where a high dose centrally is typically sought for as in the new clinical protocol in Copenhagen. In this study it is easier to evaluate the robustness of homogenous dose distributions and this was therefore used subsequently.

Table 2. The dose constraints from Copenhagen University Hospital (as previously used).

OARs	Dose constraint
Medulla	Max 18 Gy(RBE)
Lungs	Max 13 Gy(RBE) to 30% of the volume
Esophagus	Max 1 cm^3 more than 21 Gy(RBE)
Heart	Max 1 cm^3 more than 21 Gy(RBE)
Trachea	Max 21 Gy(RBE)
Bronchi	Max 30 Gy(RBE)

Because the first attempt of treatment plans did not achieve clinical accepted target coverage, a robust treatment planning was considered. The density of the entire PTV was changed to an approximate mean value of the density of the tumors, in this case 35 HU. Treatment planning was then done based on these manipulated planning CT data and the dose distributions were then recalculated to the original planning CT scan. This was considered the ground truth treatment plan. To test the robustness of the voluntary breath-hold approach the dose was then recalculated to CT scans of Day 1 to Day 3 as described further on in the section Simulation of treatment delivery.

An important assumption made in this project is that only one stable breath-hold is necessary per treatment (or a very high reproducibility of the intrafractional breath-holds). Thereby the

only motions considered in this project are the interfractional motions, since we have no information about the intrafractional motion.

4.4 DOSE CALCULATION

The dose calculation made using the treatment planning system PSIplan is divided into the following seven steps (personal communications, Tony Lomax), (Lomax *et al.*, 2004) and (Pedroni *et al.*, 1995).

1. The software creates a distance matrix in the CT scan in relation to the predefined target. The points *inside* the target get positive values and the points *outside* the targets get negative values.
2. The software calculates the water equivalent depth for all of the dose calculation points. The distance between dose calculation points can be defined by the user. As an approximation, only points in the distance of ± 3 σ from the center of the pencil beam are defined as dose calculation points, since it is time consuming to calculate the dose in the entire volume of the patient for every pencil beam. In addition, the dose outside of this distance is very low.
3. All possible positions of the Bragg peaks in the entire volume are defined. They are separated by 4.5 mm in the beam direction and 5 mm in the directions orthogonal to the beam. The possible positions of the Bragg peaks depend on the energy of the beam, and thereby the number and thickness of the range shifters, and finally also by the angle of the gantry. In this case there are 37 range shifters available made from polyethylene.
4. Next an initial set of position of the Bragg peaks is created. The software places Bragg peaks inside the target, plus a margin defined by the user of typically 5 mm from the border of the target. Initial beam weight is given to the Bragg peaks, where the distal end of the target is given the highest weights as seen from the nozzle of the gantry.
5. A first dose calculation is done. By a look-up table with the depth dose curve, the absolute dose in every dose calculation spot can be calculated. The absolute dose depth curve is achieved by measuring the relative depth dose curve and fit this to a physical model. The lateral spread is approximated to be a Gaussian distribution.
6. Next the optimization parameters are defined. Here one can for example change the number of iterations.
7. Finally an optimization (see the section Dose optimization), and a final dose calculation are performed.

4.5 DOSE OPTIMIZATION

The iterative optimization algorithm is shown in Equation 1 where χ^2 is the quadratic cost function aimed to be as small as possible, g_i the weight of the importance of the i:th dose calculation point, P the prescribed dose and D the by the treatment planning system calculated dose. By varying the weight of the importance for the dose calculation point one can aim to minimize the cost function.

Equation 1. The quadratic cost function of the optimization algorithm.

$$\chi^2 = \sum_{i=1}^{n} {g_i}^2 (P_i - D_i)^2$$

4.6 SIMULATION OF TREATMENT DELIVERY

The treatment plans are based on the beam parameters of Gantry 1 at PSI. The calculations of treatment times however consider a delivery at Gantry 2, which enables the faster scanning technique and is foreseen for the treatment of moving targets.

The initial treatment plan (Planning CT) is recalculated on the repeated CT scans (Day 1 to Day 3) after a Rigid Image Registration (RIR) of the Planning CT scan with the Day 1 to Day 3 CT scan and is performed to simulate correct positioning of the patient. For the RIR the position of the marker inside the tumor was manually brought into accordance. In a few exceptional cases the marker was invisible or had moved outside the tumor. In these cases the tumor was used to bring the images into accordance instead.

4.6.1 DEFORMABLE IMAGE REGISTRATION

To investigate the influence of non-rigid geometry changes we additionally performed "deformable dose recalculations" with two different methods and softwares. First, in the software Velocity AI 2.6.1 (Velocity Medical Solutions, U.S.A), where the initial CT scan (Planning CT) and the repeated CT scans (Day 1 to Day 3) was deformable registered to each other after which a deformable recalculation of the treatment plans was performed. This was done by using the motion fields to deform the dose matrix as described by Munck af Rosenschöld *et al.* (Munck af Rosenschold *et al.*, 2010). Finally the dose for the entire treatment was calculated by summing up the dose in each voxel for each repeated CT scan (Day 1 to Day 3). The Velocity AI uses a mixture of the algorithms B-spline and Demons for the deformable image registration. This recalculation is here referred to as DIR_velocity.

Second, in an in-house (at PSI) developed program using a demons algorithm with an affine transformation for initial alignment was employed. With the help of deformable image registration, motion vector fields between the initial CT scan (Planning CT) and the repeated CT scans (Day 1 to Day 3) were calculated. Based on these vector fields a recalculation on the deformable dose grids was performed. This approach also takes into account water equivalent path length changes due to changes in the geometry. In addition to day specific recalculations also the total dose distribution for the entire treatment was calculated. These recalculations are here referred to as DIR_demons.

The "deformable dose recalculations" can be considered more realistic than the rigid ones. However, they also come with some ambiguity since there currently do not exist perfect deformable image registration algorithms. Thus, depending on the algorithm used the results might vary slightly.

4.7 STATISTICS

A useful way of evaluating treatment plans is by inspecting the Dose Volume Histogram (DVH). A DVH is a cumulative histogram of the dose and volume of the treatment plan. By the previously delineated target volumes and OARs one can investigate the DVH for each organ or volume. In Table 3 the dose parameters are showed, used in order to compare the treatment plans in this work.

Table 3. The doses considered in this work.

Organ	Parameter
PTV	V95%
GTV	V95%
Lungs	Mean dose
Medulla	Maximum dose
Heart	Mean dose

Analyses of the data (graphs etc.) were performed in MATLAB® R2012b (8.0.0.783) (The MathWorks, Inc.).

Statistical analysis was performed with IBM SPSS® Statistics Software, Version 19 and 21 (International Business Machines Corporate (IBM), USA). By studying the deviation in the recalculated V95% in comparison to the initial V95% one could perform statistical analyses on the following topics.

- Are the two plans (2F and 3F) similar in the sense of the robustness?
- Are the analyses with RIR different from the analyses with the DIR approaches in the sense of the robustness?
- Are there correlations between the robustness and the size of the target, the initial V95% and/or the time since the planning CT scan was acquired?

The first two analyses were performed with Wilcoxon Signed-Rank tests and the last analyze was performed with regression tests for the most common models (linear, logarithmic, inverse and exponential). To determine whether the regression models were significant, F-tests were performed.

5 RESULTS

The data for all dose calculations and recalculations are shown in Appendix A – the data (RIR), Appendix B – the data (DIR_velocity) och Appendix C – the data (DIR_demons). A summary of the data is presented in the following paragraphs.

For one exemplary patient (patient 1) the initial dose distribution of the planning CT and the recalculated treatment plans (Day 1 to Day 3) are shown in Figure 4 for the three field plan (3F) using the RIR approach. One can see that the dose bath has the approximate same shape, the hot spots are in the same place and the target coverage looks similar.

The results of the DVH analyze are shown in Figure 5 for both plans (2F and 3F) using the RIR approach. The red line represents the median value, the blue box the 25th and 75th percentile, the black whiskers the range without the outliers, and the red crosses the outliers. Here one can see the dose for all target and OAR volumes (as in Table 3). The V95% for PTV for both set of plans have a range of 10-15 percentage points with a median value of 90-95%. The median value of GTV V95% was 100% with only a few percentage points as a range. The heart recieved a mean dose of less than 3% in all cases, the spinal cord a maximum dose of less than 30% and the mean dose to the lungs was always below 15%. One could conclude that there were no cases where the dose constraints to the OARs as shown in Table 2 were exceeded, with the exception of one single case where the dose constraint to the heart was slighltly exceeded in the recalculated plans (Day 1 to Day 3). One could further see that for 6/15 patients and 9/15 patients, 2F and 3F respectivetely the deviation in V95% was less than 5% during the treatment. Of all recalculated plans there were 27/41 plans and 33/41 plans 2F and 3F respectivetely, which deviated less than 5%.

In Figure 6 the PTV DVH are shown for all patients and plan 3F. In most cases the target coverage looks similar for the initial and recalculated plans, with a few exceptions.

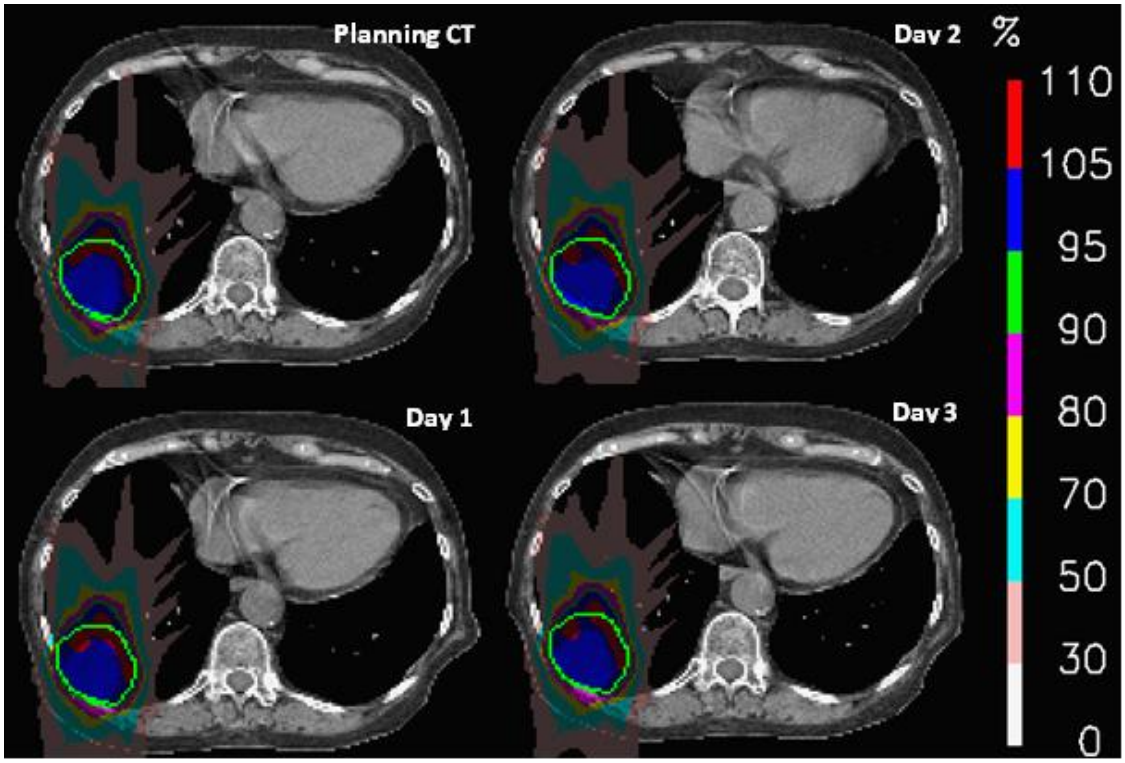

Figure 4. The dose distributions for all the treatment plans for patient 1 (3F with three fields). One can see that the dose bath has the approximate same shape, the hot spots are in the same place and the target coverage looks similar in every figure.

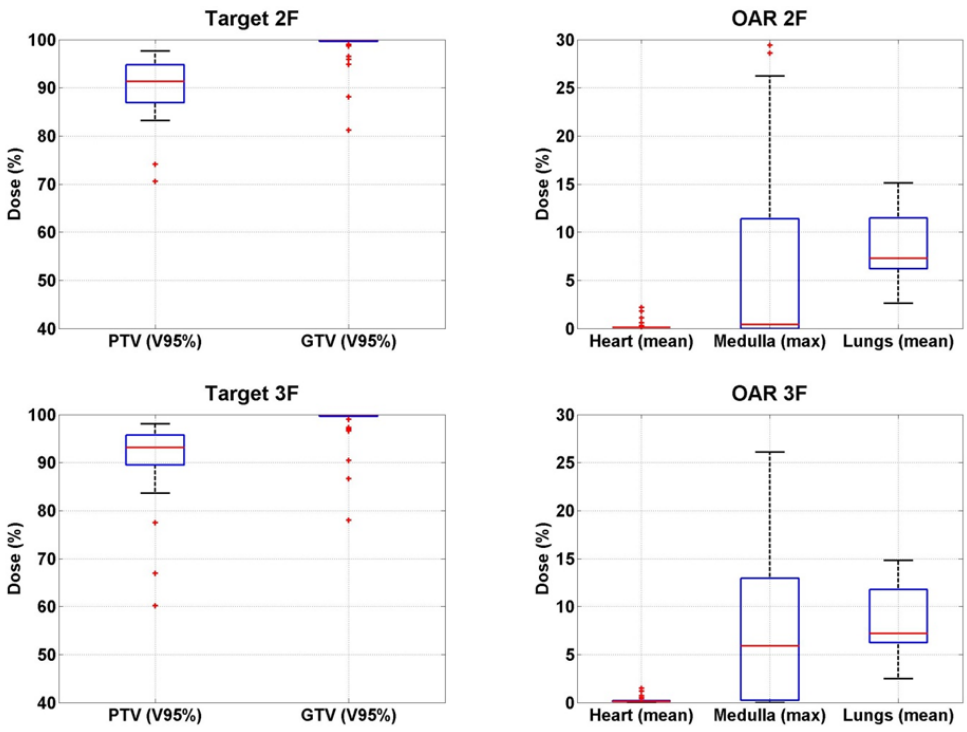

Figure 5. The descriptive statistics of the doses to the target and the OARs for the RIR approach. The top row shows the results from 2F (two fields) and the bottom row the results from 3F (three fields). The red line represents the median value, the blue box the 25th and 75th percentile, the black whiskers the range without the outliers, and the red crosses the outliers.

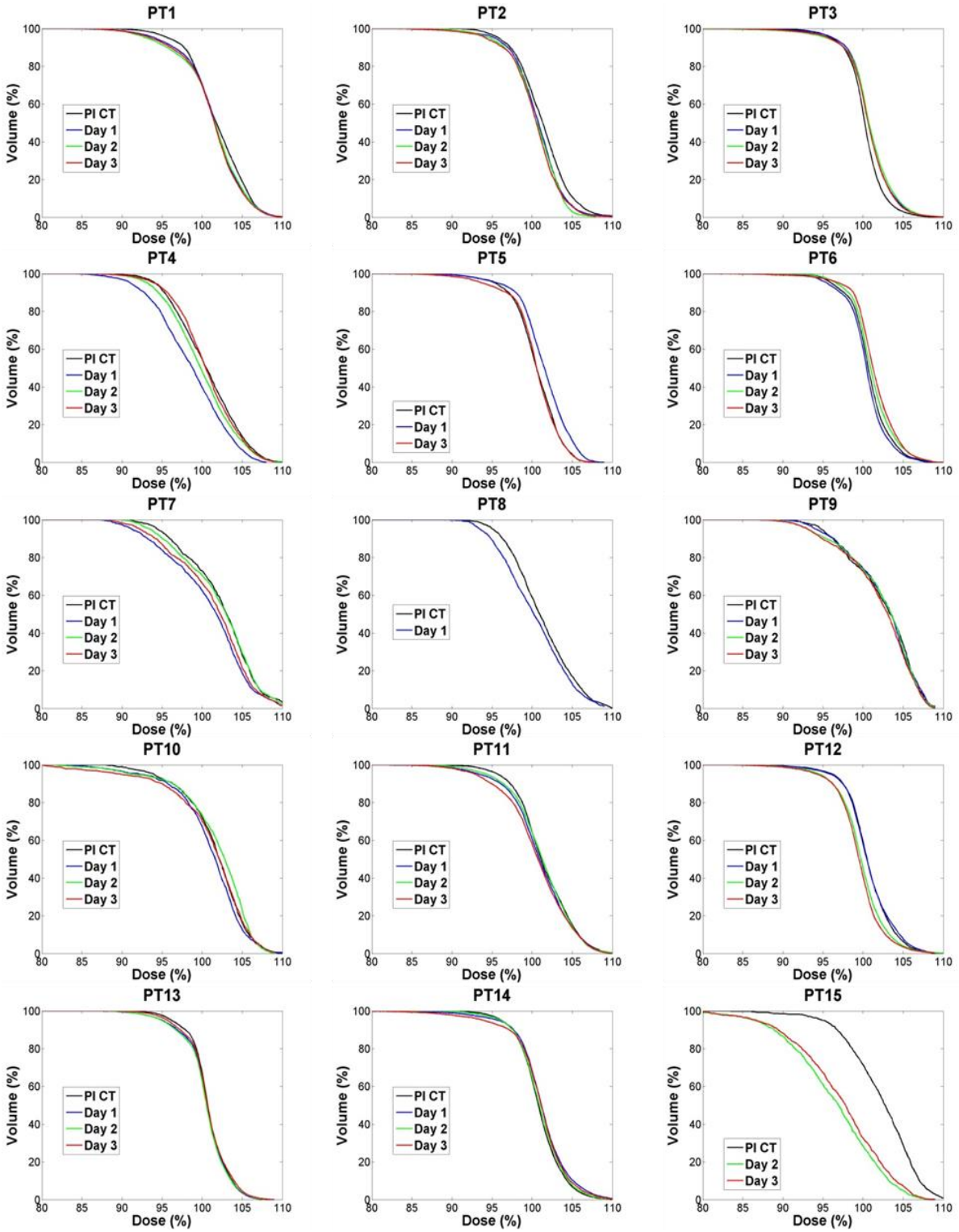

Figure 6. The Dose Volume Histogram (DVH) for the PTV, where the relative volume is shown as a function of the relative dose for all of the patients (PT) and plan 3F. The different colors represent different treatment plans where the black lines are Planning CT, the blue line Day 1, the green line Day 2 and the red line Day 3.

5.1 DEFORMABLE IMAGE REGISTRATION

In Figure 7 results of the DIR_velocity approach are shown. Because of difficulties in the data transmission of the treatment plans from "PSI format" to DICOM, the DIR_velocity recalculated plans was normalised to the mean dose of the PTV in the Planning CT treatment plan for each patient. The recalculations were only performed on the three field plan (3F), but for all patients.

The V95% for PTV for had a range of 30-35 percentage points with a median value of about 90%. The median valuue of GTV V95% was 100% with only a few percentage points in range. The heart recieved a mean dose of less than 2% in all cases, the spinal cord a maximum dose of less than 20% and the mean dose to the lungs was always below 12%. By studying the deviation in PTV V95% compared to the initial V95%, one could see that for 6/15 patients the deviation was less than 5% and for 23/41 recalculated plans it was also less than 5%. However, for the dose distribution summed over the entire treatment the number of dose distributions deviating less than 5% was 9/15.

For the DIR_demons approach only four patients (but both 2F and 3F) were studied due to the time consuming process of this image registration. The first patient was patient 1 (see Table 1), and the next two were chosen with the aim of having cases with different target sizes and location (patient 7 and 12). The last case was chosen because of large visible interfractional motion (patient 2).

The results for the 3F plan with the DIR_demons approach are shown in Figure 8. The range of the V95% for the PTV was 35-40 precentages with a median value of 90-95%. The median value of V95% was 100% with only a few percentage points in range. The heart recieved a mean dose of less than 2% in all cases, the spinal cord a maximum dose of less than 30% and the mean dose to the lungs was always below 15%. By studying the deviation from the initial V95% one could see that none of the patients had a deviation less than 5%. For all twelve recalculated cases four plans deviated less than 5% (2F and 3F). For the summed dose distribution 3/4 and 2/4 patients, 2F and 3F respectivetely had a deviation of less than 5%. Note however that for one of the patients three targets were included in this analyze which could lead to an over estimate of the dose to the OAR, compared to when only one target is included in the treatment.

In Figure 9 the DVH is shown for PTV and patient 1 both after a RIR (left) and DIR_demons (right) recalculation. The figure to the right also shows DVH for the summed dose distribution.

Additionally all the image registrations were examined visually in order to detect obvious errors in the DIR_demons process.

In conclusion, in the "deformable dose recalculations", the dose constraints of the OARs were never exceeded.

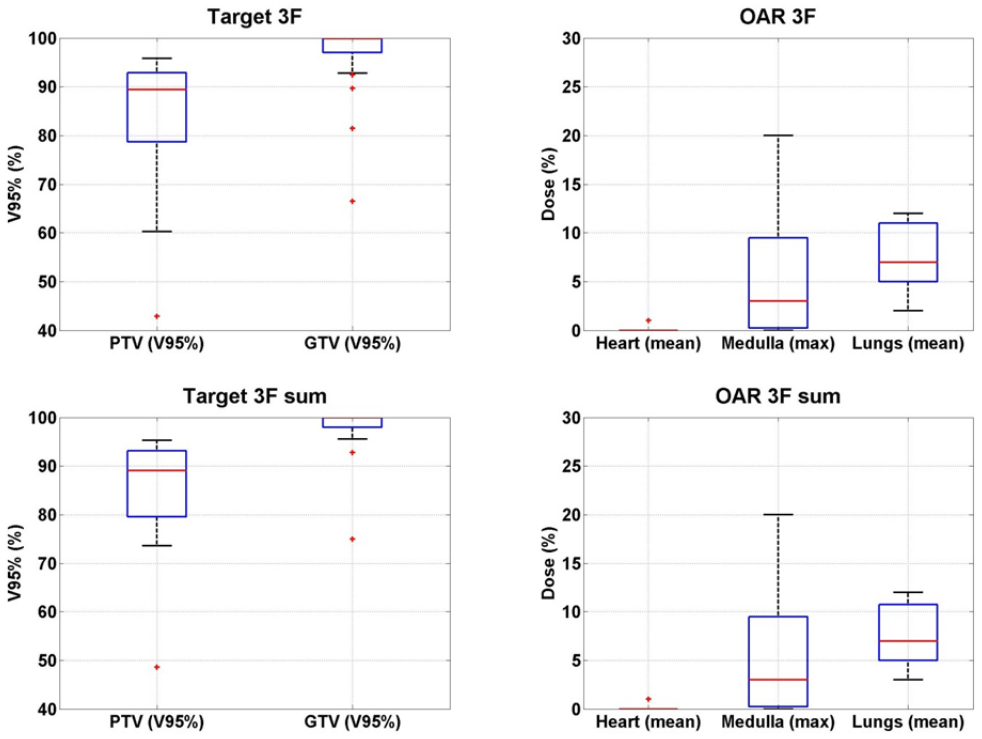

Figure 7. The descriptive statistics for the DIR_velocity approach of the target and OARs for all patients. The top row shows the results from 3F (three fields) and the bottom row the result summed over the entire treatment for 3F.

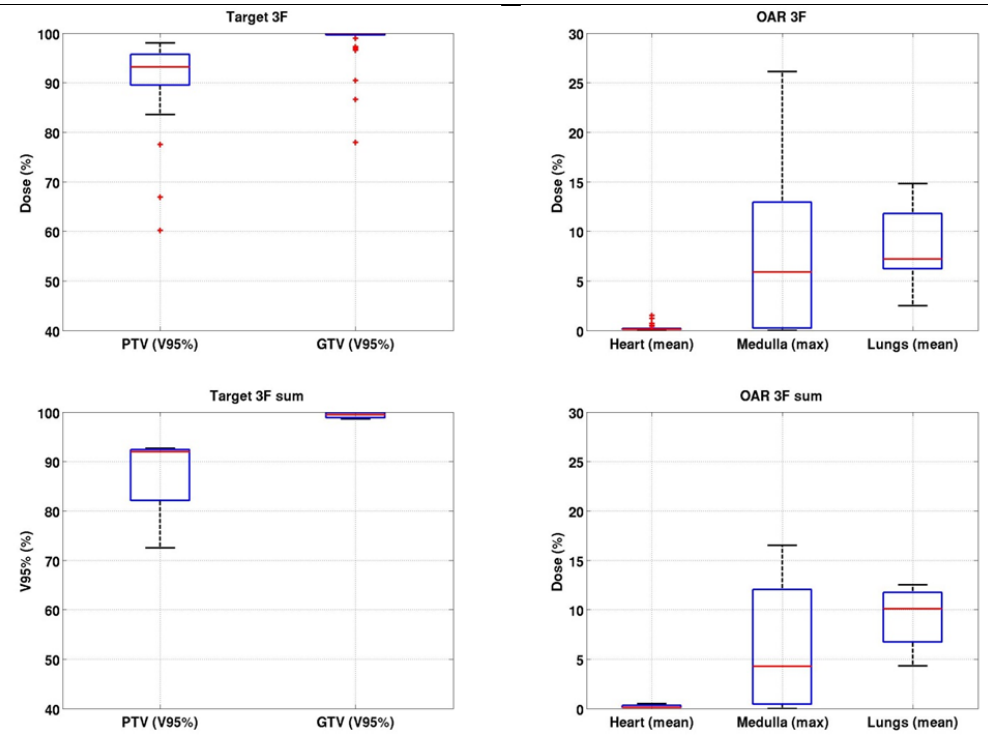

Figure 8. The descriptive statistics for the DIR_demons approach. The top row shows the result from 3F (three fields) and the bottom row shows the results summed over the entire treatment for 3F. Note that only four patients are included in this recalculation.

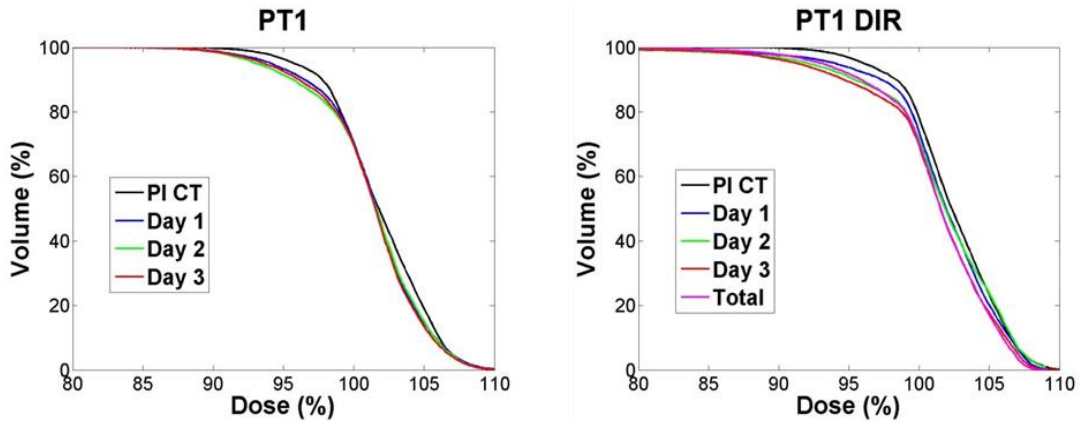

Figure 9. The dose volume histogram (DVH) for PTV and patient 1 shown for both the RIR (left) and the DIR_demons (right) approach. The black lines are the Planning CT, the blue lines Day 1, the green lines Day 2, the red lines Day3 and in the right picture only the pink line is the summed treatment.

5.2 STATISTICAL ANALYSES

In the top row in Figure 10 one can see the PTV V95% as a function of two different variables; the graph to the left as a function of the size of the target and the graph to the right as a function of the initial V95%. Figure 10 also shows the ratio of the V95% and the initial V95% as a function of the time since the planning CT scan was acquired (bottom left).

By regression tests one could see that the ratio of the V95% and the initial V95% (and thereby the robustness) was correlated with the size of the target for plans with the RIR (2F and 3F) and the DIR_velocity (3F) approach, see Appendix D – statistical analyses. The correlation showed that for increasing size of the target the ratio also increased. Further one can see in the appendix that the ratio do not correlate with the initial V95% or the time since the planning CT scan was acquired except for two cases (2F and 3F DIR_demons) where the deviation correlated with the time since the planning CT scan was acquired.

Regarding the similarities of the two plans and also between the RIR and DIR approaches, the results of these statistical analyses are also show in Appendix D – statistical analyses. One can see that the plans are alike in the sense of their robustness and that the RIR and DIR_velocity recalculations (2F and 3F) are not alike. In the latter case, the results showed that the DIR-velocity had less value of the ratios (less robust) than the RIR recalculation. By briefly studying the data of the DIR_velocity and DIR_demons approaches, no obvious differences could be detected.

All the analyses were performed with a significance level of 0.05.

5.3 TIMING

For the four patients who underwent the DIR_demons recalculations, it was also possible to simulate the total time needed to deliver a field at Gantry 2, PSI, assuming a stable beam current and no inter-logs. The results for both plans are shown in Figure 11. Here one can see that the time needed per field varied between 20s up to 100s per field for the two-field plan (2F) and varied between 10s up to 70 s per field for the three field plan (3F). The delivery time per field in general depends on the tumor size, which correlates with the number of spots needed per field, as one can see in Figure 11 and Table 1. A typical DIBH lasts 20 seconds (personal communications Gitte Persson).

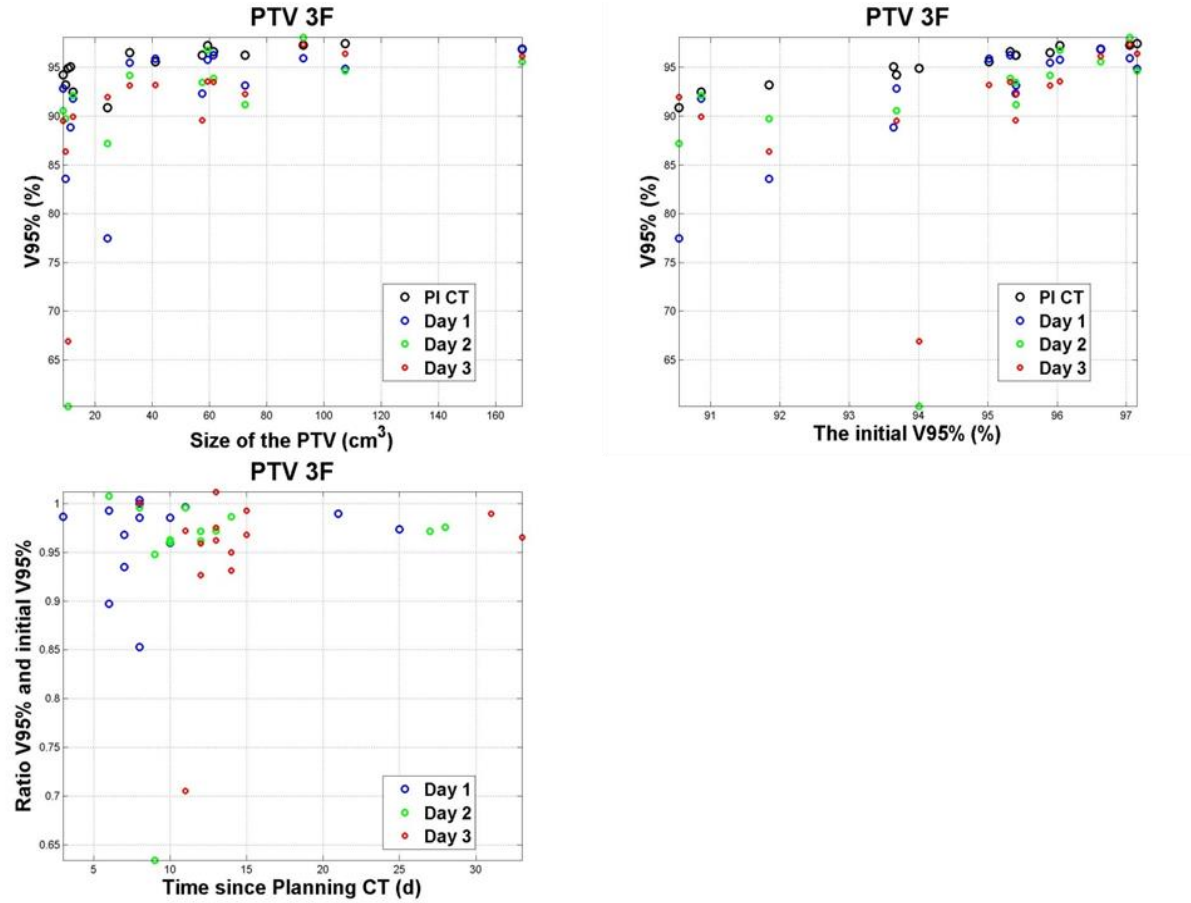

Figure 10. Top left: The PTV V95% as a function of the size of the PTV. Top right: The PTV V95% as a function of the initial V95%. Bottom left: The *ratio* of the PTV V95% and initial V95% as a function of the time since the planning CT scan was acquired. The different colors represent different treatment plans, where the black dots are Planning CT, the blue dots Day 1, the green dots Day 2 and the red dots Day 3.

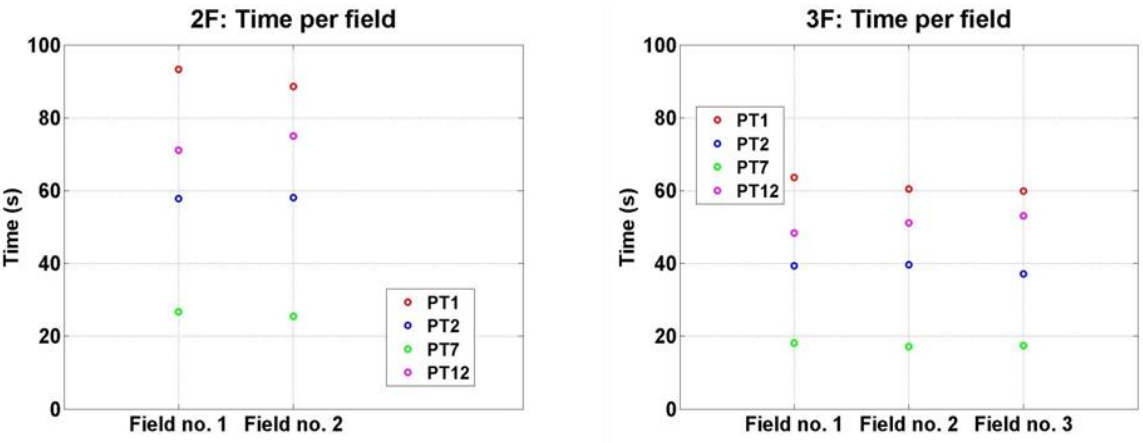

Figure 11. The time per field to deliver the treatment for 2F (two fields) and 3F (three fields). Note from Table 1 that the size of the PTV is as follows: PT1 72 cm³, PT2 32 cm³, PT7 10 cm³ and PT12 61 cm³. The different colors represent different patients where the red dos are patient 1, the blue dots patient 2, the green dots the patient 7 and the pink dots patient 12.

6 DISCUSSION

In this study the robustness of the voluntary breath-hold approach for the treatment of lung cancer with scanned proton therapy was investigated. The definition of robustness in this case was if the deviation in V95% for PTV was less than 5%. For most cases the breath-hold approach appeared to be robust.

For the cases for which the dose distribution was not robust we could either see that the target was small, or one could already in the image registration process see that the target had moved or the lung volume was different in the two images, i.e. interfractional motions. Further studies are necessary to conclude if it is possible to correlate this interfractional motion and the interfractional reproducibility of the breath-hold with the robustness of the treatment plans. Knowledge of this can provide the clinic information on selecting patients for whom this kind of motion management technique might be inappropriate to use.

For the patient with the outliers in Figure 5 one could estimate the movement of the target to be about 1 cm. As discussed before, the dose distribution to the target is smeared out when interfractional motion is present and the target coverage can be worsened. For tumors seated in the lung, the density changes can also have a severe impact to the target coverage as seen in this case because of very large density variations in and around the target (tissue, air and bone).

For some other cases where the deviation was more than 5%, there were obvious interfractional movements (change in the tumor position from one breath-hold to another; a so called baseline shift). Attempts were made to perform a more sophisticated image registration matching on the surrounding bones instead of the markers (e.g. spinal cord and rib cage). The result was slightly better, but still the deviation was more than 5%.

For the patient cases with proton plans that were not robust, we consider that possible reasons for this could be small targets ($<10 cm^3$) and/or clearly visible baseline shift (interfractional motion).

Worth mentioning is that there were actually some cases with small tumors and clearly visible interfractional movements which in fact appear to be robust. This indicates that the results for these cases are actually better than for other cases of the same kind. This topic also needs to be further investigated.

The assumption of one stable breath-hold per treatment as mentioned before may or may not be valid. It is also necessary to investigate the intrafractional motion and thereby the intrafractional reproducibility of the breath-holds and how this correlates with the robustness of the breath-hold approach.

In this study, only the target coverage was considered. The dose constraints were however met in all but one case. It could be of interest to also study the possible differences of the dose to the OARs in a way of trying to minimize the complications of the proton therapy treatment.

A brief analyze of the robustness of the treatment plans and the location of the tumors, concluded that of the cases that did not meet our robustness criterion, a majority of the tumors were located in the lower lobe. One should however also note that a majority of all tumors were located in the lower lobe. Further studies have to show if the robustness correlates with the location of the tumor, or maybe if it correlates with the motion of the tumor instead (which in turn could be correlated to the location).

6.1 DEFORMABLE IMAGE REGISTRATION

As mentioned before, for the DIR_velocity recalculation approach only the 3F plan (three fields) was studied. Since the robustness of the two plans does not seem to be different, one would not expect different result for 2F than for 3F with this approach.

In both of the DIR approaches the results for the summed dose distribtuion were better than the evalutation day by day as seen in Appendix B – the data (DIR_velocity),Appendix C – the data (DIR_demons) and also e.g. for one patient in Figure 9. This indicates that even if one treatment fraction has bad target coverage, the use of fractionation smears out the daily dose contributions and the total target coverage is better. This is an accepted fact in fractionated radiotherapy.

The robustness of the treatment with the DIR_demons recalculation showed a correlation with the time since treatment planning CT scan was acquired, but the rest of the approaches did not. One may have to be careful drawing conclusions from the DIR_demons data, since only four patients were included in that part of the study. This is a topic for further investigation.

An important question is which recalculation approach gives the most correct answer, RIR or DIR? In this study the DIR_demons approach showed slightly different result than the DIR_velocity, but no obvious large deviations was found between these two approaches. The slight difference in the two DIR analyses could be caused by the potential error in the assumption for the DIR_velocity approach (and the data transmission from PSIplan to DICOM) or the fact that for the DIR_demons approach only four patients were studied compared to the fifteen studied in the DIR_velocity approach. Generally, the DIR recalculations show in theory a more accurate dose distribution than the RIR recalculations, but the DIR algorithms may be prone to uncertainties. Zhang *et al.* performed a number of different deformable image registrations with different algorithms on the structures of the liver (Zhang *et al.*, 2012). By copying the liver structures with the DIR algorithm they could calculate the error compared to the "ground truth" (in this case the movement of implanted fiducial markers). They found an error less than 3 mm for all these deformable image registration algorithms (including the one used in this thesis, here referred to as DIR_demons). How big the uncertainty is for the DIR_velocity approach is however unclear.

One example of an error occurred during this project is shown in Figure 12 for the DIR_demons registration. The figure shows the motion fields of the image registration where the arrows indicate the direction and size of the motion needed in order for the two images to match (in this case Planning CT scan and Day 1 CT scan). In the figure to the left one can see long arrows even outside of the patient. Even though the movement of the structures outside of the patient (e.g. couch, cushion) may affect the dose distribution to the patient, it may affect the dose distribution in an inaccurate way in this DIR_demons registration and recalculation process. The density of all the structures outside of the patient was then changed to air (-1000 HU) and a new deformable image registration was performed. The motion fields of this registration are shown in the image to the right. Here one can see that the size of the arrows is much smaller than before, not only outside of the patient but also inside (the big red arrows points to examples of the motion field vectors in the image to the right). This indicates that the points outside of the patient also affect the motion fields inside the patient, which is not correct. With this in mind, and the reasoning above, the second approach with the density of the surroundings of the patents changed to air, was used throughout this project.

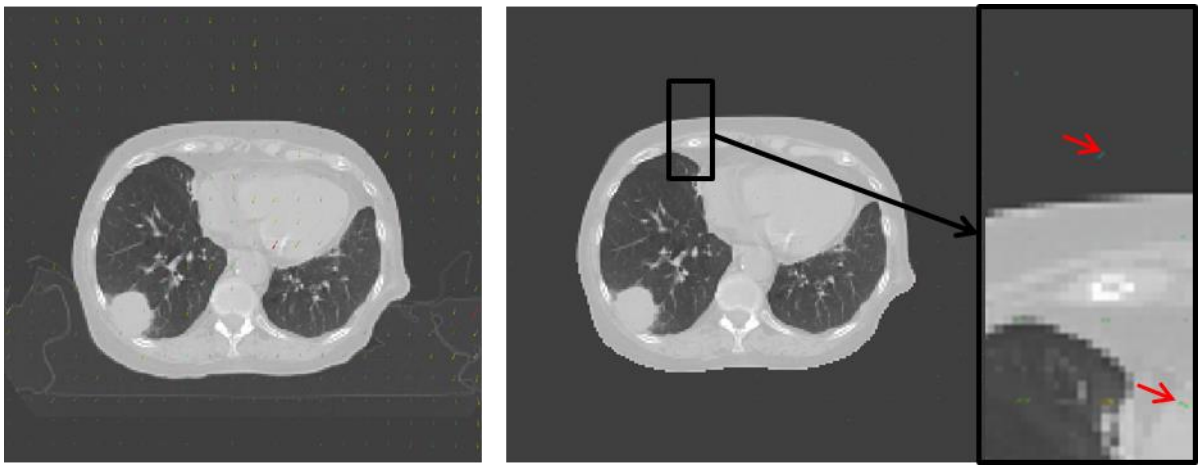

Figure 12. The motion fields of the deformable image registration for the DIR_demons approach for patient 1 (Planning CT and CT 1) performed on the original CT scans (left) and the CT scans where the density of the surroundings of the patients is changed to -1000 HU (right). The arrows (not the big red arrows) indicate the direction and the size of the motion needed in order for the images to match. Note that the arrows in the right image are smaller than the ones in the left images. In the enlarged image the big red arrows points at two examples of the motion field vectors which are very hard to detect otherwise.

6.2 THE USE OF PTV IN PROTON THERAPY

In this study we use the PTV with a 5 mm expansion in every direction from the GTV as mentioned before. The use of PTV in radiation therapy is motivated by margins accounting for physiological motion and setup errors. The concept of PTV works fine for photons, but for protons there are some additional problems. Because of possibly large range uncertainties of the protons that may also be correlated to the setup errors orthogonal to the beam, the PTV should have different appearance than the one used for photons, according to Lomax (Lomax, 2011). It is by Lomax recommended to use different expansions of the PTV in the distal and proximal part of the target, leading to one PTV per field. In passively scattered proton therapy this can be done by the use of compensators and collimators, while not using a PTV at all. In scanned proton therapy, however, Lomax further states that there is yet no optimal way to do this. In particular, most treatment planning software do not allow field-specific PTVs, so work has started to include the range uncertainty of the protons into the optimization tool of the treatment planning system (Lomax, 2011).

6.3 PROSPECTS OF THE STUDY

Apart from the already mentioned, here are some additional topics that need to be further investigated.

The robustness seems to correlate with the size of the target. It may even be necessary with a limit in size of the target in order to reassure the robustness of all treated cases. This limit needs to be further investigated.

The assumption made in this project to have one stable breath-hold per treatment fraction (or a very high reproducibility) may not be feasible as mentioned before. The fact that the voluntary breath-hold technique at all seems robust makes it possible to further investigate the technique with more realistic approaches. According to the results in Figure 11 (the time per field) it is clear that it is not possible to deliver the entire field in only one breath-hold for all patients. What was clear even before was that more than one field is not possible to deliver in one breath-hold, due to the time needed to change the position of the gantry. Now, one could start to reflect

over the reproducibility of the breath-holds. As a prospect to this study one could investigate the robustness of the breath-hold approach for a more realistic reproducibility of the breath-hold (i.e. not assume one single static breath-hold per treatment). Also interesting is to study if the robustness increases when teaching the breath-hold in advance, giving the patient audible and/or visible coaching during the treatment and also when instead using the DIBH technique as described by e.g. Hanley *et al.* (Hanley *et al.*, 1999), where the reproducibility was only a few millimeter. More generally one could investigate the possible correlation between the reproducibility of the breath-holds and the robustness of the treatment. This information could be of great importance when selecting appropriate patient cases suitable for this motion management technique. It requires some kind of measuring method of the reproducibility of the breath-holds. Currently there is an ongoing study at Rigshospitalet where the reproducibility of visually coached DIBH during a 33 fraction treatment course is investigated. Ten patients are included so far and the results look promising (personal communications Gitte Persson).

Regarding the time needed per field to deliver the treatment it should be mentioned that for some cases with small targets, only one breath-hold will be needed per field as concluded when comparing Figure 11 with the possible breath-hold times for the patients in the above mentioned study by Hanley *et al.*

It is also of interest to investigate this project using different treatment planning systems and also to compare it with Monte Carlo simulations, in a way to determine the accuracy in the treatment planning system PSIplan when calculating doses in the thorax part of the body. Comparisons with the treatment planning system and Monte Carlo simulations has been performed on previously treated cases at PSI with a satisfying accordance (Tourovsky *et al.*, 2005), but no lung cases was included in this study.

Finally, phantom studies and/or clinical studies also need to be performed before one could definitely conclude if this breath-hold approach is robust. Especially clinical studies are important where one could investigate the most important effect; the complication and survival rate of the patients undergoing proton therapy with the voluntary breath-hold approach.

7 CONCLUSIONS

The robustness of the voluntary breath-hold approach was investigated in this study and the results show that the approach is appeared to be robust for most patients. Correlations between the robustness and the size of the target could be seen, indicating that target size could be used as an inclusion criterion for the use of the treatment strategy. Further investigations of e.g. the robustness of the treatment plans when not assuming only one stable breath-hold per treatment and ways to improve the reproducibility of the breath-holds are needed. Finally also studies to show the possible correlation of the robustness of the treatment and the intra- and interfractional movements are necessary to take into account before finally deciding if this voluntary breath-hold approach is robust for the treatment of early stage lung cancer with scanned proton beam therapy.

8 REFERENCES

Cancerfonden S 2009 Populärvetenskapliga fakta om cancer: Cancer i siffror 2009

Furukawa T, Inaniwa T, Sato S, Shirai T, Mori S, Takeshita E, Mizushima K, Himukai T and Noda K 2010 Moving target irradiation with fast rescanning and gating in particle therapy *Medical Physics* **37** 4874-9

Hall E J 2006 Intensity-modulated radiation therapy, protons, and the risk of second cancers *International journal of radiation oncology, biology, physics* **65** 1-7

Hanley J, Debois M M, Mah D, Mageras G S, Raben A, Rosenzweig K, Mychalczak B, Schwartz L H, Gloeggler P J, Lutz W, Ling C C, Leibel S A, Fuks Z and Kutcher G J 1999 Deep inspiration breath-hold technique for lung tumors: the potential value of target immobilization and reduced lung density in dose escalation *International journal of radiation oncology, biology, physics* **45** 603-11

ICRU 2007 Prescribing, Recording, and Reporting Proton-Beam Therapy (ICRU Report 78) *J ICRU 2010, International Commission on Radiation Units and Measurements (ICRU) Report 78* **7**

ICRU 2010 Prescribing, Recording, and Reporting Intensity-Modulated Photon-Beam Therapy (IMRT)(ICRU Report 83) *J ICRU 2010, International Commission on Radiation Units and Measurements (ICRU) Report 83* **10** 1-106

Keall P J, Mageras G S, Balter J M, Emery R S, Forster K M, Jiang S B, Kapatoes J M, Low D A, Murphy M J, Murray B R, Ramsey C R, Van Herk M B, Vedam S S, Wong J W and Yorke E 2006 The management of respiratory motion in radiation oncology report of AAPM Task Group 76 *Med Phys* **33** 3874-900

Knopf A C, Hong T S and Lomax A 2011 Scanned proton radiotherapy for mobile targets-the effectiveness of re-scanning in the context of different treatment planning approaches and for different motion characteristics *Physics in medicine and biology* **56** 7257-71

Lomax A 1999 Intensity modulation methods for proton radiotherapy *Physics in medicine and biology* **44** 185-205

Lomax A 2011 *Proton Therapy Physics*: CRC Press) pp 335-80

Lomax A J, Bohringer T, Bolsi A, Coray D, Emert F, Goitein G, Jermann M, Lin S, Pedroni E, Rutz H, Stadelmann O, Timmermann B, Verwey J and Weber D C 2004 Treatment planning and verification of proton therapy using spot scanning: initial experiences *Med Phys* **31** 3150-7

Miller D W 1995 A review of proton beam radiation therapy *Med Phys* **22** 1943-54

Munck af Rosenschold P, Aznar M C, Nygaard D E, Persson G F, Korreman S S, Engelholm S A and Nystrom H 2010 A treatment planning study of the potential of geometrical tracking for intensity modulated proton therapy of lung cancer *Acta oncologica (Stockholm, Sweden)* **49** 1141-8

Paul Scherrer Institut P 2013-05-02 PSI Webpage www.psi.ch

Pedroni E, Bacher R, Blattmann H, Bohringer T, Coray A, Lomax A, Lin S, Munkel G, Scheib S, Schneider U and et al. 1995 The 200-MeV proton therapy project at the Paul Scherrer Institute: conceptual design and practical realization *Med Phys* **22** 37-53

Persson G F 2011 Uncertainties in target definition for radiotherapy of peripheral lung tumoure *Dan Med Bull* **58** B4314

Persson G F, Josipovic M, Nygaard D E, Recke P, Aznar M, Juhler-Nottrup T, Rosenschold P M, Korreman S and Specht L 2013 Percutaneously implanted markers in peripheral lung tumours: Report of complications *Acta oncologica (Stockholm, Sweden)* **52** 1225-8

Phillips M H, Pedroni E, Blattmann H, Boehringer T, Coray A and Scheib S 1992 Effects of respiratory motion on dose uniformity with a charged particle scanning method *Physics in medicine and biology* **37** 223-34

Robertson J M, Ten Haken R K, Hazuka M B, Turrisi A T, Martel M K, Pu A T, Littles J F, Martinez F J, Francis I R, Quint L E and Lichter A S 1997 Dose escalation for non-small cell lung cancer using conformal radiation therapy *International journal of radiation oncology, biology, physics* **37** 1079-85

Rosenzweig K E, Hanley J, Mah D, Mageras G, Hunt M, Toner S, Burman C, Ling C C, Mychalczak B, Fuks Z and Leibel S A 2000 The deep inspiration breath-hold technique in the treatment of inoperable non-small-cell lung cancer *International journal of radiation oncology, biology, physics* **48** 81-7

Schippers M 2011 *Proton Therapy Physics*: CRC Press) pp 61-102

Siegel R, Naishadham D and Jemal A 2013 Cancer statistics, 2013 *CA: a cancer journal for clinicians* **63** 11-30

Tourovsky A, Lomax A J, Schneider U and Pedroni E 2005 Monte Carlo dose calculations for spot scanned proton therapy *Physics in medicine and biology* **50** 971-81

van de Water S, Kreuger R, Zenklusen S, Hug E and Lomax A J 2009 Tumour tracking with scanned proton beams: assessing the accuracy and practicalities *Physics in medicine and biology* **54** 6549-63

Vasquez A C, Runz A, Echner G, Sroka-Perez G and Karger C P 2012 Comparison of two respiration monitoring systems for 4D imaging with a Siemens CT using a new dynamic breathing phantom *Physics in medicine and biology* **57** N131-43

Zhang Y, Boye D, Tanner C, Lomax A J and Knopf A 2012 Respiratory liver motion estimation and its effect on scanned proton beam therapy *Physics in medicine and biology* **57** 1779-95

Zuofeng L, Roelf S, Stella F and Daniel K Y 2011 *Proton Therapy Physics*: CRC Press) pp 221-64

9 APPENDIX A – THE DATA (RIR)

Below are the data for all patients for the RIR recalculation shown. In the table the doses to the volumes previously mentioned are shown together with the doses that can help to decide whether the dose constraints are exceeded or not (see Table 2 and Table 3). Note that in one case, the dose to the heart was too high (highlighted with red color).

Patient	CT	Plan	PTV	GTV	Heart		Medulla	Lung sin		Lung dx		Lung sum	
			V95% (%)	V95% (%)	Mean (%)	V47% (ccm)	Max (%)	Mean (%)	V30% (%)	Mean (%)	V30 (%)	Mean (%)	V30% (%)
1	Pl. CT	2 fields	95,41	100	0,8	0,1	0	0,1	0	9,9	14,27	10	14,27
		3 fields	96,23	100	0,6	0	0	0,1	0	10,8	14,92	10,9	14,92
	Day 1	2 fields	90,37	99,88	1,1	0,23	0	0,1	0	9,8	14,22	9,9	14,22
		3 fields	93,14	100	0,7	0	0	0,1	0	10,8	14,95	10,9	14,95
	Day 2	2 fields	89,41	99,97	0,6	0	0	0,1	0	9,5	13,78	9,6	13,78
		3 fields	91,21	100	0,4	0	0	0,1	0	10,4	13,85	10,5	13,85
	Day 3	2 fields	89,95	100	0,6	0	0	0,1	0	9,7	13,97	9,8	13,97
		3 fields	92,28	100	0,4	0	0	0,1	0	10,8	14,8	10,9	14,8
Patient	CT	Plan	PTV	GTV	Heart		Medulla	Lung sin		Lung dx		Lung sum	
			V95% (%)	V95% (%)	Mean (%)	V47% (ccm)	Max (%)	Mean (%)	V30% (%)	Mean (%)	V30 (%)	Mean (%)	V30% (%)
2	Pl. CT	2 fields	95,9	100	0,1	0	0,4	8,3	11,85	0,1	0	8,4	11,85
		3 fields	96,52	100	0,1	0	0,3	7,5	10,17	0,1	0	7,6	10,17
	Day 1	2 fields	90,41	100	0,1	0	0,4	9	13,11	0,1	0	9,1	13,11
		3 fields	95,5	100	0,1	0	0,3	8,6	11,52	0,1	0	8,7	11,52
	Day 2	2 fields	91,68	100	0,1	0	0,4	8,7	12,85	0,1	0	8,8	12,85
		3 fields	94,17	100	0,1	0	0,3	8	11,28	0,1	0	8,1	11,28
	Day 3	2 fields	88,7	100	0,1	0	0,4	8,9	12,95	0,1	0	9	12,95
		3 fields	93,14	100	0,1	0	0,3	8,5	11,56	0,1	0	8,6	11,56
Patient	CT	Plan	PTV	GTV	Heart		Medulla	Lung sin		Lung dx		Lung sum	
			V95% (%)	V95% (%)	Mean (%)	V47% (ccm)	Max (%)	Mean (%)	V30% (%)	Mean (%)	V30 (%)	Mean (%)	V30% (%)
3	Pl. CT	2 fields	96,63	99,94	0,1	0	27,3	0,1	0	14,2	20,15	14,3	20,15
		3 fields	96,89	99,91	0,1	0	18,7	0,1	0	13,8	19,86	13,9	19,86
	Day 1	2 fields	96,17	100	0,1	0	16,4	0,1	0	13,8	19,42	13,9	19,42
		3 fields	96,89	100	0,1	0	11,3	0,1	0	13,3	18,65	13,4	18,65
	Day 2	2 fields	94,89	99,97	0,1	0	10,7	0,1	0	13,2	18,57	13,3	18,57
		3 fields	95,59	99,99	0,1	0	7,1	0,1	0	12,7	17,54	12,8	17,54
	Day 3	2 fields	95,55	100	0,1	0	15,1	0,1	0	13,4	18,88	13,5	18,88
		3 fields	96,15	100	0,1	0	10	0,1	0	13	18,2	13,1	18,2
Patient	CT	Plan	PTV	GTV	Heart		Medulla	Lung sin		Lung dx		Lung sum	
			V95% (%)	V95% (%)	Mean (%)	V47% (ccm)	Max (%)	Mean (%)	V30% (%)	Mean (%)	V30 (%)	Mean (%)	V30% (%)
4	Pl. CT	2 fields	90,54	99,38	0,1	0	0,1	0,1	0	6,9	10,24	7	10,24
		3 fields	90,87	99,13	0,1	0	4,8	0,3	0	6,8	10,1	7,1	10,1
	Day 1	2 fields	86,1	96,53	0,1	0	0,3	0,1	0	6,7	10,04	6,8	10,04
		3 fields	77,48	90,45	0,1	0	6,5	0,6	0,08	6,6	9,94	7,2	10,02
	Day 2	2 fields	86,82	99,01	0,1	0	0,1	0,1	0	6,8	10,13	6,9	10,13
		3 fields	87,22	97,27	0,1	0	3,4	0,2	0	6,7	9,76	6,9	9,76
	Day 3	2 fields	91,75	100	0,1	0	0,2	0,1	0	6,8	10,09	6,9	10,09
		3 fields	91,95	99,75	0,1	0	4,8	0,2	0	6,7	9,82	6,9	9,82
Patient	CT	Plan	PTV	GTV	Heart		Medulla	Lung sin		Lung dx		Lung sum	
			V95% (%)	V95% (%)	Mean (%)	V47% (ccm)	Max (%)	Mean (%)	V30% (%)	Mean (%)	V30 (%)	Mean (%)	V30% (%)
5	Pl. CT	2 fields	95,02	100	0,1	0	0	0,1	0	12,9	15,03	13	15,03
		3 fields	95,59	100	0,1	0	27,5	0,1	0	11,8	15,8	11,9	15,8
	Day 1	2 fields	94,77	100	0,1	0	0	0,1	0	12,6	14,9	12,7	14,9
		3 fields	95,91	100	0,1	0	22,4	0,1	0	11,6	15,79	11,7	15,79
	Day 3	2 fields	88,71	99,88	0,1	0	0	0,1	0	12,7	14,98	12,8	14,98
		3 fields	93,22	100	0,1	0	22,2	0,1	0	11,7	16,07	11,8	16,07
Patient	CT	Plan	PTV	GTV	Heart		Medulla	Lung sin		Lung dx		Lung sum	
			V95% (%)	V95% (%)	Mean (%)	V47% (ccm)	Max (%)	Mean (%)	V30% (%)	Mean (%)	V30 (%)	Mean (%)	V30% (%)
6	Pl. CT	2 fields	97,05	100	0,1	0	30,3	0,4	0,5	10,5	15,85	10,9	16,35
		3 fields	97,3	100	0,1	0	26,6	0,3	0,14	11,5	16,3	11,8	16,44
	Day 1	2 fields	95,78	99,93	0,1	0	29,4	0,4	0,46	10,7	16,18	11,1	16,64
		3 fields	95,95	100	0,1	0	26,1	0,3	0,19	11,7	17,01	12	17,2
	Day 2	2 fields	97,66	100	0,1	0	28,6	0,3	0,29	9,8	14,3	10,1	14,59
		3 fields	98,04	100	0,1	0	25,4	0,2	0,04	10,6	14,3	10,8	14,34
	Day 3	2 fields	96,87	100	0,1	0	26,2	0,3	0,32	9	12,67	9,3	12,99
		3 fields	97,33	100	0,1	0	23,3	0,2	0,05	9,7	12,53	9,9	12,58
Patient	CT	Plan	PTV	GTV	Heart		Medulla	Lung sin		Lung dx		Lung sum	
			V95% (%)	V95% (%)	Mean (%)	V47% (ccm)	Max (%)	Mean (%)	V30% (%)	Mean (%)	V30 (%)	Mean (%)	V30% (%)
7	Pl. CT	2 fields	91,84	97,95	0,1	0	5,3	4,7	6,82	0,1	0	4,8	6,82
		3 fields	93,19	97,6	0,1	0	3,5	4,2	5,52	0,1	0	4,3	5,52
	Day 1	2 fields	83,21	94,86	0,1	0	8,9	4,7	6,75	0,1	0	4,8	6,75
		3 fields	83,59	96,58	0,1	0	5,9	4,2	5,48	0,1	0	4,3	5,48
	Day 2	2 fields	90,02	96,58	0,1	0	6,2	4,7	6,74	0,1	0	4,8	6,74
		3 fields	89,73	96,58	0,1	0	4,1	4,2	5,49	0,1	0	4,3	5,49
	Day 3	2 fields	84,26	95,89	0,1	0	7,2	4,6	6,55	0,1	0	4,7	6,55
		3 fields	86,37	96,92	0,1	0	4,8	4,1	5,25	0,1	0	4,2	5,25

Patient	CT	Plan	PTV	GTV	Heart		Medulla	Lung sin		Lung dx		Lung sum	
			V95% (%)	V95% (%)	Mean (%)	V47% (ccm)	Max (%)	Mean (%)	V30% (%)	Mean (%)	V30 (%)	Mean (%)	V30% (%)
8	Pl. CT	2 fields	93,64	100	0,1	0	4,2	6	8,37	0,1	0	6,1	8,37
		3 fields	95,04	100	0,1	0	2,8	5,3	6,96	0,1	0	5,4	6,96
	Day 1	2 fields	83,8	99,66	0,1	0	11,4	6,1	8,63	0,1	0	6,2	8,63
		3 fields	88,84	98,98	0,1	0	7,6	5,4	7,22	0,1	0	5,5	7,22
Patient	CT	Plan	PTV	GTV	Heart		Medulla	Lung sin		Lung dx		Lung sum	
			V95% (%)	V95% (%)	Mean (%)	V47% (ccm)	Max (%)	Mean (%)	V30% (%)	Mean (%)	V30 (%)	Mean (%)	V30% (%)
9	Pl. CT	2 fields	93,68	100	0,1	0	0	0,1	0	2,8	3,81	2,9	3,81
		3 fields	94,22	100	0,1	0	0	0,1	0	2,7	3,04	2,8	3,04
	Day 1	2 fields	92,29	100	0,1	0	0	0,1	0	2,7	3,71	2,8	3,71
		3 fields	92,83	100	0,1	0	0	0,1	0	2,6	2,84	2,7	2,84
	Day 2	2 fields	90,15	100	0,1	0	0	0,1	0	2,6	3,55	2,7	3,55
		3 fields	90,58	100	0,1	0	0	0,1	0	2,5	2,79	2,6	2,79
	Day 3	2 fields	87,15	100	0,1	0	0	0,1	0	2,5	3,34	2,6	3,34
		3 fields	89,51	100	0,1	0	0	0,1	0	2,4	2,51	2,5	2,51
Patient	CT	Plan	PTV	GTV	Heart		Medulla	Lung sin		Lung dx		Lung sum	
			V95% (%)	V95% (%)	Mean (%)	V47% (ccm)	Max (%)	Mean (%)	V30% (%)	Mean (%)	V30 (%)	Mean (%)	V30% (%)
10	Pl. CT	2 fields	90,86	100	0,1	0	12	0,1	0	4,6	6,18	4,7	6,18
		3 fields	92,5	100	0,1	0	8	0,1	0	4,4	4,91	4,5	4,91
	Day 1	2 fields	91,72	100	0,1	0	11,5	0,1	0	4,7	6,17	4,8	6,17
		3 fields	91,8	100	0,1	0	7,6	0,1	0	4,4	5,03	4,5	5,03
	Day 2	2 fields	89,45	100	0,1	0	11,8	0,1	0	4,3	5,48	4,4	5,48
		3 fields	92,11	100	0,1	0	7,8	0,1	0	4,2	5,05	4,3	5,05
	Day 3	2 fields	85,94	100	0,1	0	11,5	0,1	0	4,6	6,08	4,7	6,08
		3 fields	89,92	100	0,1	0	7,6	0,1	0	4,4	5,23	4,5	5,23
Patient	CT	Plan	PTV	GTV	Heart		Medulla	Lung sin		Lung dx		Lung sum	
			V95% (%)	V95% (%)	Mean (%)	V47% (ccm)	Max (%)	Mean (%)	V30% (%)	Mean (%)	V30 (%)	Mean (%)	V30% (%)
11	Pl. CT	2 fields	95,4	99,88	0,9	0	2,1	0,1	0	11	16,23	11,1	16,23
		3 fields	96,24	100	0,6	0	1,4	0,1	0	11,6	14,9	11,7	14,9
	Day 1	2 fields	91,29	99,77	2,2	3,41	2,4	0,1	0	11,7	17,67	11,8	17,67
		3 fields	92,34	99,96	1,5	0	1,6	0,1	0	12,6	17,1	12,7	17,1
	Day 2	2 fields	92,98	99,96	1,7	1,9	2,3	0,1	0	11,2	16,82	11,3	16,82
		3 fields	93,48	100	1,2	0	1,5	0,1	0	11,8	15,24	11,9	15,24
	Day 3	2 fields	89,52	99,61	1,8	1,82	2,1	0,1	0	11,5	17,36	11,6	17,36
		3 fields	89,6	100	1,2	0	1,4	0,1	0	12,3	16,57	12,4	16,57
Patient	CT	Plan	PTV	GTV	Heart		Medulla	Lung sin		Lung dx		Lung sum	
			V95% (%)	V95% (%)	Mean (%)	V47% (ccm)	Max (%)	Mean (%)	V30% (%)	Mean (%)	V30 (%)	Mean (%)	V30% (%)
12	Pl. CT	2 fields	95,32	99,89	0,1	0	0	0,1	0	9,4	10,65	9,5	10,65
		3 fields	96,63	100	0,1	0	15,5	0,1	0	9	11,81	9,1	11,81
	Day 1	2 fields	95,99	100	0,1	0	0	0,1	0	9,4	10,66	9,5	10,66
		3 fields	96,28	100	0,1	0	11,9	0,1	0	9	11,8	9,1	11,8
	Day 2	2 fields	93,68	99,64	0,1	0	0	0,1	0	9,3	10,64	9,4	10,64
		3 fields	93,9	99,75	0,1	0	16,5	0,1	0	8,9	11,76	9	11,76
	Day 3	2 fields	91,89	98,63	0,1	0	0	0,1	0	9,2	10,62	9,3	10,62
		3 fields	93,53	99,6	0,1	0	18,2	0,1	0	8,9	11,8	9	11,8
Patient	CT	Plan	PTV	GTV	Heart		Medulla	Lung sin		Lung dx		Lung sum	
			V95% (%)	V95% (%)	Mean (%)	V47% (ccm)	Max (%)	Mean (%)	V30% (%)	Mean (%)	V30 (%)	Mean (%)	V30% (%)
13	Pl. CT	2 fields	97,15	100	0,7	0	19,1	0,1	0	7,3	11,11	7,4	11,11
		3 fields	97,46	100	0,4	0	12,7	0,1	0	8,1	11,28	8,2	11,28
	Day 1	2 fields	93,42	99,8	0,3	0	20,2	0,1	0	5,9	8,26	6	8,26
		3 fields	94,87	100	0,2	0	13,4	0,1	0	6,5	7,02	6,6	7,02
	Day 2	2 fields	93,72	99,91	0,2	0	19,9	0,1	0	5,8	7,85	5,9	7,85
		3 fields	94,65	100	0,1	0	13,2	0,1	0	6,1	6,62	6,2	6,62
	Day 3	2 fields	95,4	99,96	0,2	0	20	0,1	0	6,1	8,74	6,2	8,74
		3 fields	96,41	100	0,2	0	13,3	0,1	0	6,6	7,16	6,7	7,16
Patient	CT	Plan	PTV	GTV	Heart		Medulla	Lung sin		Lung dx		Lung sum	
			V95% (%)	V95% (%)	Mean (%)	V47% (ccm)	Max (%)	Mean (%)	V30% (%)	Mean (%)	V30 (%)	Mean (%)	V30% (%)
14	Pl. CT	2 fields	96,04	99,59	0,1	0	1,1	7,1	10,73	0,1	0	7,2	10,73
		3 fields	97,22	99,69	0,6	0	0,7	6,8	10,57	0,1	0	6,9	10,57
	Day 1	2 fields	95,29	100	0,1	0	0,2	6,6	9,94	0,1	0	6,7	9,94
		3 fields	95,8	100	0,5	0	0,1	6,3	9,55	0,1	0	6,4	9,55
	Day 2	2 fields	95,57	99,87	0,1	0	0,1	6,8	10,22	0,1	0	6,9	10,22
		3 fields	96,78	99,91	0,6	0	0,1	6,5	9,92	0,1	0	6,6	9,92
	Day 3	2 fields	93,87	100	0,1	0	0,1	6,4	9,58	0,1	0	6,5	9,58
		3 fields	93,55	100	0,5	0	0,1	6,1	9,15	0,1	0	6,2	9,15
Patient	CT	Plan	PTV	GTV	Heart		Medulla	Lung sin		Lung dx		Lung sum	
			V95% (%)	V95% (%)	Mean (%)	V47% (ccm)	Max (%)	Mean (%)	V30% (%)	Mean (%)	V30 (%)	Mean (%)	V30% (%)
15	Pl. CT	2 fields	94,01	98,56	0,1	0	1,4	3,8	5,37	0,1	0	3,9	5,37
		3 fields	94,91	100	0,1	0	0,9	3,5	4,67	0,1	0	3,6	4,67
	Day 2	2 fields	70,57	81,23	0,1	0	0,3	3,8	5,5	0,1	0	3,9	5,5
		3 fields	60,22	77,98	0,1	0	0,2	3,5	4,88	0,1	0	3,6	4,88
	Day 3	2 fields	74,11	88,09	0,1	0	0	3,7	5,28	0,1	0	3,8	5,28
		3 fields	66,94	86,64	0,1	0	0	3,4	4,65	0,1	0	3,5	4,65

10 APPENDIX B – THE DATA (DIR_VELOCITY)

Below are the data for all patients for the DIR_velocity recalculation shown for 3F with three fields. In the table the doses to the volumes previously mentioned are shown together with the doses that can help to decide whether the dose constraints are exceeded or not (see Table 2 and Table 3).

Patient	CT	Plan	PTV	GTV	Heart		Medulla	Lung sin		Lung dx		Lung sum	
			V95% (%)	V95% (%)	Mean (%)	V47% (ccm)	Max (%)	Mean (%)	V30% (%)	Mean (%)	V30 (%)	Mean (%)	V30 (%)
1	Pl. CT	2 fields											
		3 fields	92,19	100	0	0	0	0	0	11	15,09	11	15,09
	Day 1	2 fields											
		3 fields	91,26	99,97	1	0	0	0	0	11	15,42	11	15,42
	Day 2	2 fields											
		3 fields	87,76	100	0	0	0	0	0	11	13,27	11	13,27
	Day 3	2 fields											
		3 fields	85,89	99,84	0	0	0	0	0	11	15,2	11	15,2
	Sum	2 fields											
		3 fields	89,07	100	0	0	0	0	0	11	14,57	11	14,57
Patient	CT	Plan	PTV	GTV	Heart		Medulla	Lung sin		Lung dx		Lung sum	
			V95% (%)	V95% (%)	Mean (%)	V47% (ccm)	Max (%)	Mean (%)	V30% (%)	Mean (%)	V30 (%)	Mean (%)	V30 (%)
2	Pl. CT	2 fields											
		3 fields	91,27	100	0	0	0	8	10,4	0	0	8	10,4
	Day 1	2 fields										0	
		3 fields	80,25	97,69	0	0	0	6	8,52	0	0	6	8,52
	Day 2	2 fields											
		3 fields	71,42	92,42	0	0	1	7	9,43	0	0	7	9,43
	Day 3	2 fields											
		3 fields	74,49	94,68	0	0	0	7	9,34	0	0	7	9,34
	Sum	2 fields											
		3 fields	73,58	95,58	0	0	1	7	8,78	0	0	7	8,78
Patient	CT	Plan	PTV	GTV	Heart		Medulla	Lung sin		Lung dx		Lung sum	
			V95% (%)	V95% (%)	Mean (%)	V47% (ccm)	Max (%)	Mean (%)	V30% (%)	Mean (%)	V30 (%)	Mean (%)	V30 (%)
3	Pl. CT	2 fields											
		3 fields	96,91	100	0	0	14	0	0	14	20,04	14	20,04
	Day 1	2 fields											
		3 fields	95,58	100	0	0	9	0	0	13	18,18	13	18,18
	Day 2	2 fields											
		3 fields	92,65	99,97	0	0	6	0	0	12	16,54	12	16,54
	Day 3	2 fields											
		3 fields	92,1	99,9	0	0	12	0	0	12	17,32	12	17,32
	Sum	2 fields											
		3 fields	93,36	99,97	0	0	8	0	0	12	17,34	12	17,34
Patient	CT	Plan	PTV	GTV	Heart		Medulla	Lung sin		Lung dx		Lung sum	
			V95% (%)	V95% (%)	Mean (%)	V47% (ccm)	Max (%)	Mean (%)	V30% (%)	Mean (%)	V30 (%)	Mean (%)	V30 (%)
4	Pl. CT	2 fields											
		3 fields	90,99	100	0	0	2	0	0	7	10,07	7	10,07
	Day 1	2 fields											
		3 fields	82,63	95,91	0	0	1	1	0,08	6	9,7	7	9,78
	Day 2	2 fields											
		3 fields	94,59	99,02	0	0	3	0	0	7	9,72	7	9,72
	Day 3	2 fields											
		3 fields	92,62	99,84	0	0	5	0	0	6	9,54	6	9,54
	Sum	2 fields											
		3 fields	91,35	98,6	0	0	3	0	0	6	9,52	6	9,52
Patient	CT	Plan	PTV	GTV	Heart		Medulla	Lung sin		Lung dx		Lung sum	
			V95% (%)	V95% (%)	Mean (%)	V47% (ccm)	Max (%)	Mean (%)	V30% (%)	Mean (%)	V30 (%)	Mean (%)	V30 (%)
5	Pl. CT	2 fields											
		3 fields	96,31	100	0	0	23	0	0	12	16,17	12	16,17
	Day 1	2 fields											
		3 fields	95,81	100	0	0	19	0	0	11	15,7	11	15,7
	Day 3	2 fields											
		3 fields	92,95	100	0	0	20	0	0	12	16,1	12	16,1
	Sum	2 fields											
		3 fields	95,07	100	0	0	20	0	0	12	15,77	12	15,77
Patient	CT	Plan	PTV	GTV	Heart		Medulla	Lung sin		Lung dx		Lung sum	
			V95% (%)	V95% (%)	Mean (%)	V47% (ccm)	Max (%)	Mean (%)	V30% (%)	Mean (%)	V30 (%)	Mean (%)	V30 (%)
6	Pl. CT	2 fields											
		3 fields	92,11	100	0	0	19	0	0,09	12	16,62	12	16,71
	Day 1	2 fields											
		3 fields	91,31	100	0	0	16	0	0,16	12	17,11	12	17,27
	Day 2	2 fields											
		3 fields	94,82	100	0	0	14	0	0,02	11	14,86	11	14,88
	Day 3	2 fields											
		3 fields	94,14	100	0	0	10	0	0,02	10	13,09	10	13,11
	Sum	2 fields											
		3 fields	94,46	100	0	0	14	0	0,01	11	14,61	11	14,62
Patient	CT	Plan	PTV	GTV	Heart		Medulla	Lung sin		Lung dx		Lung sum	
			V95% (%)	V95% (%)	Mean (%)	V47% (ccm)	Max (%)	Mean (%)	V30% (%)	Mean (%)	V30 (%)	Mean (%)	V30 (%)
7	Pl. CT	2 fields											
		3 fields	86,91	93,78	0	0	0	4	5,19	0	0	4	5,19
	Day 1	2 fields											
		3 fields	72,96	89,64	0	0	2	4	5,05	0	0	4	5,05
	Day 2	2 fields											
		3 fields	84	92,75	0	0	1	4	5,04	0	0	4	5,04
	Day 3	2 fields											
		3 fields	78,57	93,78	0	0	1	4	4,72	0	0	4	4,72
	Sum	2 fields											
		3 fields	76,46	92,75	0	0	1	4	5,03	0	0	4	5,03

Patient	CT	Plan	PTV	GTV	Heart		Medulla	Lung sin		Lung dx		Lung sum	
			V95% (%)	V95% (%)	Mean (%)	V47% (ccm)	Max (%)	Mean (%)	V30% (%)	Mean (%)	V30 (%)	Mean (%)	V30 (%)
8	Pl. CT	2 fields											
		3 fields	91,6	100	0	0	1	5	6,98	0	0	5	6,98
	Day 1	2 fields											
		3 fields	88,37	100	0	0	3	5	7,41	0	0	5	7,41
	Sum	2 fields											
		3 fields	88,37	100	0	0	3	5	7,41	0	0	5	7,41
Patient	CT	Plan	PTV	GTV	Heart		Medulla	Lung sin		Lung dx		Lung sum	
			V95% (%)	V95% (%)	Mean (%)	V47% (ccm)	Max (%)	Mean (%)	V30% (%)	Mean (%)	V30 (%)	Mean (%)	V30 (%)
9	Pl. CT	2 fields											
		3 fields	88,01	100	0	0	0	0	0	3	3,05	3	3,05
	Day 1	2 fields											
		3 fields	86,11	100	0	0	0	0	0	3	2,81	3	2,81
	Day 2	2 fields											
		3 fields	87,79	100	0	0	0	0	0	3	2,73	3	2,73
	Day 3	2 fields											
		3 fields	87,11	100	0	0	0	0	0	2	2,54	2	2,54
	Sum	2 fields											
		3 fields	85,58	100	0	0	0	0	0	3	2,6	3	2,6
Patient	CT	Plan	PTV	GTV	Heart		Medulla	Lung sin		Lung dx		Lung sum	
			V95% (%)	V95% (%)	Mean (%)	V47% (ccm)	Max (%)	Mean (%)	V30% (%)	Mean (%)	V30 (%)	Mean (%)	V30 (%)
10	Pl. CT	2 fields											
		3 fields	87,6	100	0	0	6	0	0	4	4,72	4	4,72
	Day 1	2 fields											
		3 fields	85,69	100	0	0	3	0	0	5	5,38	5	5,38
	Day 2	2 fields											
		3 fields	87,58	100	0	0	4	0	0	4	5,16	4	5,16
	Day 3	2 fields											
		3 fields	74,65	96,76	0	0	5	0	0	5	5,49	5	5,49
	Sum	2 fields											
		3 fields	82,28	100	0	0	4	0	0	5	5,13	5	5,13
Patient	CT	Plan	PTV	GTV	Heart		Medulla	Lung sin		Lung dx		Lung sum	
			V95% (%)	V95% (%)	Mean (%)	V47% (ccm)	Max (%)	Mean (%)	V30% (%)	Mean (%)	V30 (%)	Mean (%)	V30 (%)
11	Pl. CT	2 fields											
		3 fields	92,6	99,87	1	0	1	0	0	12	14,64	12	14,64
	Day 1	2 fields											
		3 fields	78,7	97,66	1	0	2	0	0	11	13,83	11	13,83
	Day 2	2 fields											
		3 fields	84,52	99,91	1	0	1	0	0	10	12,19	10	12,19
	Day 3	2 fields											
		3 fields	78,66	98,09	1	0	1	0	0	11	13,68	11	13,68
	Sum	2 fields											
		3 fields	78,65	97,77	1	0	2	0	0	10	13	10	13
Patient	CT	Plan	PTV	GTV	Heart		Medulla	Lung sin		Lung dx		Lung sum	
			V95% (%)	V95% (%)	Mean (%)	V47% (ccm)	Max (%)	Mean (%)	V30% (%)	Mean (%)	V30 (%)	Mean (%)	V30 (%)
12	Pl. CT	2 fields											
		3 fields	96,79	100	0	0	10	0	0	9	12,1	9	12,1
	Day 1	2 fields											
		3 fields	91,7	100	0	0	8	0	0	9	11,46	9	11,46
	Day 2	2 fields											
		3 fields	91,09	99,96	0	0	11	0	0	9	11,76	9	11,76
	Day 3	2 fields											
		3 fields	89,45	99,75	0	0	14	0	0	9	12,12	9	12,12
	Sum	2 fields											
		3 fields	90,96	99,83	0	0	10	0	0	9	11,78	9	11,78
Patient	CT	Plan	PTV	GTV	Heart		Medulla	Lung sin		Lung dx		Lung sum	
			V95% (%)	V95% (%)	Mean (%)	V47% (ccm)	Max (%)	Mean (%)	V30% (%)	Mean (%)	V30 (%)	Mean (%)	V30 (%)
13	Pl. CT	2 fields											
		3 fields	94,27	100	0	0	14	0	0	8	11,4	8	11,4
	Day 1	2 fields											
		3 fields	95,3	100	0	0	14	0	0	8	8,33	8	8,33
	Day 2	2 fields											
		3 fields	94,68	100	0	0	11	0	0	6	6,67	6	6,67
	Day 3	2 fields											
		3 fields	94,93	100	0	0	15	0	0	7	7,33	7	7,33
	Sum	2 fields											
		3 fields	95,31	100	0	0	13	0	0	7	7,16	7	7,16
Patient	CT	Plan	PTV	GTV	Heart		Medulla	Lung sin		Lung dx		Lung sum	
			V95% (%)	V95% (%)	Mean (%)	V47% (ccm)	Max (%)	Mean (%)	V30% (%)	Mean (%)	V30 (%)	Mean (%)	V30 (%)
14	Pl. CT	2 fields											
		3 fields	95,55	99,84	1	0	0	7	10,16	0	0	7	10,16
	Day 1	2 fields											
		3 fields	94,56	100	0	0	0	6	9,92	0	0	6	9,92
	Day 2	2 fields											
		3 fields	93,49	100	0	0	0	6	9,92	0	0	6	9,92
	Day 3	2 fields											
		3 fields	90,24	99,72	0	0	0	6	9,3	0	0	6	9,3
	Sum	2 fields											
		3 fields	92,32	100	0	0	0	6	9,5	0	0	6	9,5
Patient	CT	Plan	PTV	GTV	Heart		Medulla	Lung sin		Lung dx		Lung sum	
			V95% (%)	V95% (%)	Mean (%)	V47% (ccm)	Max (%)	Mean (%)	V30% (%)	Mean (%)	V30 (%)	Mean (%)	V30 (%)
15	Pl. CT	2 fields											
		3 fields	89,06	98,03	0	0	1	4	4,64	0	0	4	4,64
	Day 2	2 fields											
		3 fields	42,87	66,53	0	0	0	3	4,54	0	0	3	4,54
	Day 3	2 fields											
		3 fields	60,24	81,46	0	0	0	3	4,81	0	0	3	4,81
	Sum	2 fields											
		3 fields	48,62	74,97	0	0	0	3	4,63	1	0	4	4,63

11 APPENDIX C – THE DATA (DIR_DEMONS)

Below are the data for all patients for the DIR_demons recalculation shown. In the table the doses to the volumes previously mentioned are shown together with the doses that can help to decide whether the dose constraints are exceeded or not (see Table 2 and Table 3). Note that only four patients are included.

Patient	CT	Plan	PTV	GTV	Heart		Medulla	Lung sin		Lung dx		Lung sum	
			V95% (%)	V95% (%)	Mean (%)	V47% (ccm)	Max (%)	Mean (%)	V30% (%)	Mean (%)	V30 (%)	Mean (%)	V30 (%)
1	Pl. CT	2 fields	96	100	0,8	0,1	0	0,1	0	9,9	14,3	10	14,3
		3 fields	96,66	100	0,6	0	0	0,1	0	10,9	15	11	15
	Day 1	2 fields	93,23	100	0,9	0	0	0,1	0	9,9	14,2	10	14,2
		3 fields	93,61	100	0,6	0	0	0,1	0	10,9	14,76	11	14,76
	Day 2	2 fields	90,25	100	0,6	0	0	0,1	0	9,8	14,14	9,9	14,14
		3 fields	90,62	100	0,4	0	0	0,1	0	10,7	14,23	10,8	14,23
	Day 3	2 fields	88,81	100	0,8	0	0	0,1	0	10,1	14,43	10,2	14,43
		3 fields	89,15	100	0,6	0	0	0,1	0	11,2	15,51	11,3	15,51
	Sum	2 fields	91,37	100	0,8	0	0	0,1	0	9,9	14,27	10	14,27
		3 fields	91,74	100	0,5	0	0	0,1	0	10,9	14,52	11	14,52
Patient	CT	Plan	PTV	GTV	Heart		Medulla	Lung sin		Lung dx		Lung sum	
			V95% (%)	V95% (%)	Mean (%)	V47% (ccm)	Max (%)	Mean (%)	V30% (%)	Mean (%)	V30 (%)	Mean (%)	V30 (%)
2*	Pl. CT	2 fields	96,18	100	0,1	0	0,6	11,9	16,1	2,7	3,89	14,6	19,99
		3 fields	92,5	100	0,1	0	0,2	10,9	15,11	2,6	1,13	13,5	16,24
	Day 1	2 fields	79,64	99,92	0,1	0	0,2	9,3	12,68	2,1	3,24	11,4	15,92
		3 fields	80,04	100	0,1	0	0,1	10,2	13,54	1,9	0,56	12,1	14,1
	Day 2	2 fields	68	68	0,1	0	1,5	12	16,69	2,2	3,22	14,2	19,91
		3 fields	64,87	89,26	0,1	0	0,9	11,3	16,08	2,3	0,89	13,6	16,97
	Day 3	2 fields	79,24	99,27	0,1	0	0,1	9,2	12,58	2	3,2	11,2	15,78
		3 fields	79,14	99,03	0,1	0	0	10,2	13,59	1,9	0,45	12,1	14,04
	Sum	2 fields	75,48	99,6	0,1	0	1,7	10,1	14	2,1	2,88	12,2	16,88
		3 fields	72,5	99,11	0,1	0	0,9	10,5	13,94	2	0,62	12,5	14,56
Patient	CT	Plan	PTV	GTV	Heart		Medulla	Lung sin		Lung dx		Lung sum	
			V95% (%)	V95% (%)	Mean (%)	V47% (ccm)	Max (%)	Mean (%)	V30% (%)	Mean (%)	V30 (%)	Mean (%)	V30 (%)
7	Pl. CT	2 fields	92,42	98,29	0,1	0	5,3	4,7	6,83	0,1	0	4,8	6,83
		3 fields	93,95	98,29	0,1	0	3,5	4,2	5,54	0,1	0	4,3	5,54
	Day 1	2 fields	87,24	96,58	0,1	0	5,8	4,8	6,98	0,1	0	4,9	6,98
		3 fields	88,39	98,63	0,1	0	3,8	4,3	5,57	0,1	0	4,4	5,57
	Day 2	2 fields	88,87	97,26	0,1	0	2,6	4,6	6,67	0,1	0	4,7	6,67
		3 fields	91,84	97,25	0,1	0	1,7	4,2	5,3	0,1	0	4,3	5,3
	Day 3	2 fields	86,37	99,32	0,1	0	4	4,6	6,62	0,1	0	4,7	6,62
		3 fields	89,54	99,32	0,1	0	2,6	4,1	5,19	0,1	0	4,2	5,19
	Sum	2 fields	91,17	98,29	0,1	0	3,9	4,6	6,81	0,1	0	4,7	6,81
		3 fields	92,61	98,63	0,1	0	7,6	4,2	5,31	0,1	0	4,3	5,31
Patient	CT	Plan	PTV	GTV	Heart		Medulla	Lung sin		Lung dx		Lung sum	
			V95% (%)	V95% (%)	Mean (%)	V47% (ccm)	Max (%)	Mean (%)	V30% (%)	Mean (%)	V30 (%)	Mean (%)	V30 (%)
12	Pl. CT	2 fields	96,12	100	0,1	0	0	0,1	0	9,4	10,68	9,5	10,68
		3 fields	96,83	100	0,1	0	15,5	0,1	0	9,1	11,85	9,2	11,85
	Day 1	2 fields	94,39	99,96	0,1	0	0	0,1	0	9,4	10,68	9,5	10,68
		3 fields	94,17	99,96	0,1	0	10,9	0,1	0	9,1	11,84	9,2	11,84
	Day 2	2 fields	91,79	99,39	0,1	0	0	0,1	0	9,3	10,55	9,4	10,55
		3 fields	90,43	99,57	0,1	0	16,6	0,1	0	8,9	11,69	9	11,69
	Day 3	2 fields	90,56	99,1	0,1	0	0	0,1	0	9,6	11,04	9,7	11,04
		3 fields	90,93	99,6	0,1	0	25,4	0,1	0	9,3	12,26	9,4	12,26
	Sum	2 fields	92,67	99,57	0,1	0	0	0,1	0	9,4	10,79	9,5	10,79
		3 fields	92,2	99,71	0,1	0	16,5	0,1	0	9,1	11,93	9,2	11,93

*Note that three target was included in this treatment, leading to an over estimate of the dose to the OAR as compared to when only one target is treated.

12 APPENDIX D – STATISTICAL ANALYSES

Below are the statistical analyses shown, as performed in the software SPSS. A significance level of 0.05 was used throughout these studies. Positive correlation means in this case that the ratio (and thereby also the robustness) increases for increasing value of the parameter. In the table the regression test is referred to as Reg and Wilcoxon Signed-Rank test as Wil.

Test	Data	Parameters	Hypothesis	Curve	F*/Z**	ρ	Result
Reg.	RIR 2F	Size	No correlation	Loga-rithmic	9.7	0.003	Positive correlation
Reg.	RIR 3F	Size	No correlation	Loga-rithmic Invers	8.2 8.3	0.007 0.007	Positive correlation
Reg.	DIR_velocity	Size	No correlation	Loga-rithmic	4.8	0.034	Positive correlation
Reg.	RIR 2F	Initial V95%	No correlation	Linear	0.92	0.34	No correlation
Reg.	RIR 3F	Initial V95%	No correlation	Linear	1.8	0.19	No correlation
Reg.	DIR_velocity	Initial V95%	No correlation	Linear	2.8	0.1	No correlation
Reg.	RIR 2F	Time	No correlation	Inverse	0.2	0.6	No correlation
Reg.	RIR 3F	Time	No correlation	Linear***	0.57	0.46	No correlation
Reg.	DIR_velocity	Time	No correlation	Inverse	0.71	0.41	No correlation
Reg.	DIR_demons 2F	Size	No correlation	Linear***	0.80	0.39	No correlation
Reg.	DIR_demons 3F	Size	No correlation	Inverse	0.40	0.54	No correlation
Reg.	DIR_demons 2F	Initial V95%	No correlation	Linear***	0.99	0.34	No correlation
Reg.	DIR_demons 3F	Initial V95%	No correlation	Inverse	6.2	0.032	No correlation
Reg.	DIR_demons 2F	Time	No correlation	Linear	27	0.0	Negative correlation
Reg.	DIR_demons 3F	Time	No correlation	Linear	17	0.002	Negative correlation
Wil.	RIR	2F, 3F	No difference		-1.3	0.21	No difference
Wil.	3F	RIR, DIR_velocity	No difference		-2.1	0.038	Difference, DIR<RIR

*F is calculated for the Log regression test.
**Z is calculated for the Wilcox Signed-Rank test.
***When only the most common curve fits were considered (linear, logarithmic, inverse, exponential).